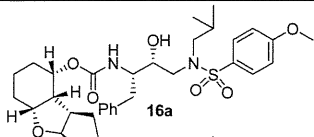
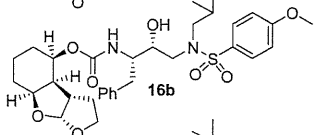
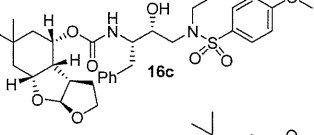
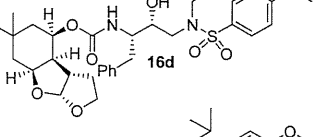
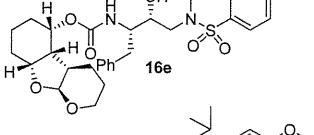
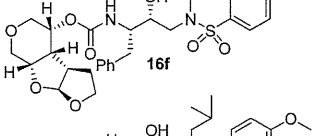
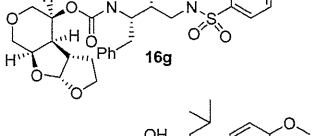
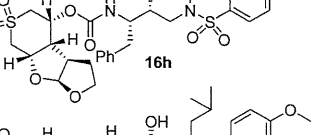
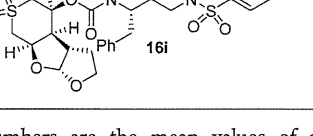


**Table 1. Structures and Potency of HIV-1 Protease Inhibitors 16a–i**

Entry	Inhibitor	$K_i$ (nM)	$IC_{50}$ ( $\mu$ M) <sup>a,b</sup>
1.		0.01	0.0019
2.		0.45	0.24
3.		8.8	nt
4.		139	nt
5.		0.41	0.048
6.		0.021	0.0045
7.		3.1	0.26
8.		0.6	>1
9.		10.5	>1

<sup>a</sup>The numbers are the mean values of at least two experiments.

<sup>b</sup>Human T-lymphoid (MT-2) cells ( $2 \times 10^3$ ) were exposed to 100 TCID<sub>50</sub> of HIV-1LAI and were cultured in the presence of each PI. IC<sub>50</sub> values were determined using the MTT assay. The IC<sub>50</sub> values of amprenavir (APV), saquinavir (SQV), indinavir (IDV), and darunavir (DRV) were 30, 15, 30, and 3 nM, respectively. Nt, not tested.

inhibitor **1**. Incorporation of a gem-dimethyl group at the C2 position resulted in inhibitors **16c** and **16d** that showed a drastic loss of enzyme affinity, possibly because of steric repulsion between the dimethyl and side-chain residues within the S2 subsite of the HIV protease. We have also investigated the effects of the 6–5–6 fused ring system over the 6–5–5 ring system. As shown, replacement of the tetrahydrofuran ring in **16a** with a tetrahydropyran ring resulted in inhibitor **16e** ( $K_i$  =

0.41 nM, antiviral IC<sub>50</sub> = 48 nM, entry 5), which showed a significant reduction in both enzyme inhibitory and antiviral activity over **16a**. We have explored the substitution of the C3-methylene group with an oxygen atom or with a sulfone functionality. Interestingly, pyran (oxygen)-substituted inhibitor **16f** ( $K_i$  = 21 pM, antiviral IC<sub>50</sub> = 4.5 nM, entry 6) with a 4(*R*)-configuration displayed comparable enzyme inhibitory and antiviral potency to that of **16a**. Consistent with the cyclohexyl derivatives, the corresponding enantiomerically pure ligand in inhibitor **16g** showed a substantial reduction in potency. Further substitution of the C2 methylene with a polar sulfone functionality resulted in a drastic reduction in enzymatic activity and antiviral potency (inhibitors **16h,i**, entries 8 and 9).

Because of the potent enzyme inhibitory and antiviral properties of inhibitors **16a** and **16f**, we selected these inhibitors for further evaluation against a panel of multidrug-resistant (MDR) HIV-1 variants. The antiviral activities of these inhibitors were compared to clinically available PIs, DRV, and amprenavir (APV),<sup>4,28</sup> and the results are shown in Table 2. Both inhibitors **16a** and **16f** exhibited low-nanomolar EC<sub>50</sub> values against the wild type.

HIV-1<sub>ERS104pre</sub> is a laboratory strain isolated from a drug-naïve patient.<sup>28</sup> Inhibitor **16a** had the most potent activity (EC<sub>50</sub> = 3.6 nM), which was similar to that of DRV and nearly 10-fold better than that of APV. Interestingly, inhibitor **16f**, with its cyclohexane ring replaced with a 3-tetrahydropyran ring, showed a 2-fold reduction in antiviral potency compared to inhibitor **16a**.

Inhibitor **16a** was tested against a panel of multidrug-resistant HIV-1 strains, and the EC<sub>50</sub> of **16a** remained in the low-nanomolar value range (8–16 nM), with fold-changes in its activity being similar to those observed for DRV.<sup>4,28</sup> In contrast, inhibitor **16f** displayed 4- and 6-fold reductions in antiviral activity against viral strains C and G compared to **16a**. Although inhibitors **16a** and **16f** both displayed a superior profile compared to another approved PI, APV, overall, inhibitor **16a** maintained impressive potency against all tested multidrug-resistant HIV-1 strains. It compared favorably with DRV, a leading PI for the treatment of multidrug-resistant HIV infection.<sup>10</sup>

To gain molecular insights into the ligand-binding site interactions responsible for the potent activity and excellent resistant profile of **16a**, we have determined the X-ray crystal structure of the HIV wild-type protease cocrystallized with **16a**, as described for DRV.<sup>29</sup> The structure was refined at a 1.29 Å resolution to an *R* factor of 0.14. The structure comprises the protease dimer and the inhibitor bound in two orientations related by a twofold rotation with 55/45% relative occupancies. The protease dimer is similar to that in the protease–DRV complex with an rmsd of 0.11 Å on all C $\alpha$  atoms.<sup>30</sup> Inhibitor **16a**'s binding elements are similar to those of inhibitor **1**.<sup>7,8</sup> The inhibitor makes extensive interactions in the HIV-1 protease active site and most notably displays favorable polar interactions, including hydrogen bonds and weaker C–H $\cdots$ O and C–H $\cdots$  $\pi$  interactions, as shown in Figure 2.

It is bound in the active-site cavity through a series of hydrogen-bond interactions and weaker CH $\cdots$ O interactions with the main-chain atoms of the HIV-1 protease. The inhibitor hydroxyl group interacts with all four carboxylate oxygen atoms of the catalytic Asp25 and Asp25', with interatomic distances of 2.6–3.2 Å. A tetracoordinated water (not labeled in the figure) mediates hydrogen bonds with both NH atoms of the flap

Table 2. Comparison of the Antiviral Activity of 16a, 16f, APV, and DRV against Multidrug-Resistant HIV-1 Variants

virus	EC <sub>50</sub> ± SD, (μM) (fold change) <sup>a,b</sup>			
	16a	16f	APV	DRV
HIV-1 <sub>104pre</sub> (wt)	0.0036 ± 0.0004	0.0083 ± 0.0021	0.028 ± 0.006	0.0037 ± 0.0007
HIV-1 <sub>MDR/C</sub>	0.008 ± 0.005 (2)	0.0329 ± 0.0030 (4)	0.325 ± 0.055 (12)	0.010 ± 0.002 (3)
HIV-1 <sub>MDR/G</sub>	0.012 ± 0.009 (3)	0.0795 ± 0.0018 (10)	0.426 ± 0.012 (16)	0.019 ± 0.005 (5)
HIV-1 <sub>MDR/TM</sub>	0.016 ± 0.001 (4)		0.448 ± 0.050 (16)	0.024 ± 0.008 (6)

<sup>a</sup>The amino acid substitutions identified in the protease-encoding region of HIV-1<sub>ERS104pre</sub> (wild type), HIV-1<sub>MDR/C</sub>, HIV-1<sub>MDR/G</sub>, and HIV-1<sub>MDR/TM</sub> compared to the consensus type B sequence cited from the Los Alamos database include L63P; L10I, I15V, K20R, L24I, M36I, M46L, I54V, I62V, L63P, K70Q, V82A, L89M; L10I, V11I, T12E, I15V, L19I, R41K, M46L, L63P, A71T, V82A, L90M; and L10I, K14R, R41K, M46L, I54V, L63P, A71V, V82A, L90M, I93L, respectively. HIV-1<sub>ERS104pre</sub> served as a source of wild-type HIV-1. <sup>b</sup>The EC<sub>50</sub> values were determined using PHA-PBMCs as target cells, and the inhibition of p24 Gag protein production by each drug was used as an end point. The numbers in parentheses represent the fold changes of the EC<sub>50</sub> values for each isolate compared to the EC<sub>50</sub> values for wild-type HIV-1<sub>ERS104pre</sub>. All assays were conducted in duplicate, and the data shown represent mean values (±1 standard deviations) derived from the results of two or three independent experiments.

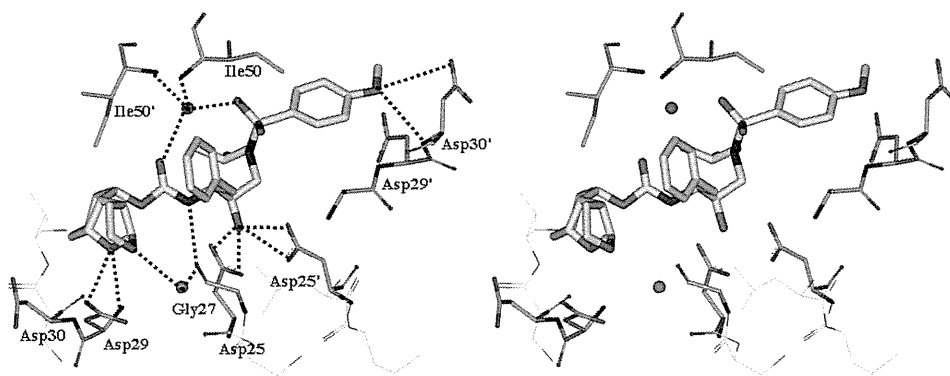


Figure 2. Stereoview of the X-ray structure of inhibitor 16a-bound HIV-1 protease (PDB code: 4KB9). All strong hydrogen-bonding interactions are shown as dotted lines.

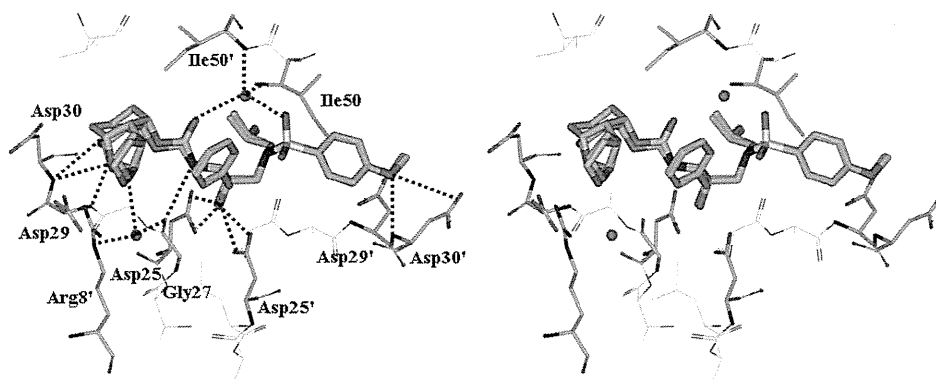


Figure 3. Stereoview of the overlay X-ray structures of inhibitor 16a (green)-bound HIV-1 protease (PDB code: 4KB9) and 1 (magenta)-bound HIV-1 protease (PDB code: 3OK9). All strong hydrogen bonding interactions of inhibitor 1 are shown as dotted lines.

residues Ile50/50' as well as the inhibitor's urethane carbonyl and one of the sulfonamide (SO<sub>2</sub>) oxygens. The oxygen atom (OMe) of sulfonamide isostere in the P2' position forms a hydrogen bond with the amide NH of Asp30' at 3.3 Å. The hydrogen bond between the inhibitor urethane amide and the carbonyl oxygen atom of Gly27 is 3.3 Å in length. The cyclohexane ring appeared to fill in the hydrophobic pocket surrounding the Ile47, Val32, Ile84, Leu76, and Ile50' residues. The tetrahydrofuran ring oxygen forms a hydrogen bond with the backbone amide NH of Asp29. The carboxylate group of Asp29 also forms a hydrogen bond with the ring oxygen of the first tetrahydrofuran ring. The protease-inhibitor interaction is further stabilized by the water-mediated hydrogen bond of the Gly27 carbonyl oxygen with the second tetrahydrofuran oxygen

of the P2 group. An overlay of the X-ray structures of 16a-bound HIV-1 protease and inhibitor 1-bound HIV-1 protease is shown in Figure 3. The binding elements of inhibitor 16a are similar to inhibitor 1 with a tris-THF P2 ligand, with the exception of cyclohexane replacing the first tetrahydrofuran ring in the P2 ligand. It appears that the first THF ring oxygen in inhibitor 1 is involved in hydrogen bonding with the backbone amide NH of Asp30 in the S2 subsite. This hydrogen-bond interaction is absent in inhibitor 16a, where the cyclohexyl ring appeared to fill in the S2 subsite. As shown in Table 2, the resistance profile of 16a can be compared favorably with DRV. However, it should be noted that inhibitor 1 displayed significantly improved antiviral potency over DRV against a variety of multidrug-resistant clinical HIV-1 strains.<sup>7</sup> The

additional backbone interactions of tris-THF ligand in inhibitor 1 may be responsible for the improved resistance profile of inhibitor 1 over DRV.

## CONCLUSIONS

We have designed a number of syn-anti-syn-fused tricyclic derivatives as P2 ligands in the S2 subsite. The P2 ligands were first synthesized stereoselectively in racemic form. The enzymatic resolution of these racemic alcohols provided rapid access to optically active ligand alcohols. Various substituents at the C2-methylene position were investigated to enhance interaction in the active site. The synthesis of the ligands was carried out using either Mn(OAc)<sub>3</sub>-based annulation or a rhodium carbenoid cycloaddition reaction as the key step. Inhibitor 16a, with a stereochemically defined fused cyclohexyl hexahydrofurofuran derivative, displayed remarkable enzyme inhibitory and antiviral potency. Inhibitor 16a has also shown excellent activity against multi-PI-resistant variants compared to other FDA approved inhibitors. A protein–ligand X-ray structure of 16a-bound HIV-1 protease was determined at a 1.29 Å resolution. The inhibitor appeared to make extensive interactions throughout the active site. Of particular interest, the cyclohexane ring appeared to nicely pack the hydrophobic pocket, and the first tetrahydrofuran oxygen forms a strong hydrogen bond with the backbone amide NH of Asp29. Also, the second tetrahydrofuran ring oxygen forms a water-mediated hydrogen bond with the Gly27 carbonyl oxygen and with a carboxylate oxygen atom of Asp29. These extensive interactions with the HIV-1 protease active site may be responsible for inhibitor 16a's potent antiviral activity and drug-resistance profiles. Further design and optimization of inhibitors utilizing this molecular insight are in progress.

## EXPERIMENTAL SECTION

**General Methods.** All anhydrous solvents were obtained according to the following procedures: diethyl ether and tetrahydrofuran (THF) were distilled from sodium/benzophenone under argon and dichloromethane from calcium hydride. All other solvents were reagent grade. All moisture-sensitive reactions were carried out in a flame-dried flask under a nitrogen atmosphere. Column chromatography was performed with Whatman 240–400 mesh silica gel under low pressure at 3–5 psi. Thin-layer chromatography was carried out with E. Merck silica gel 60-F-254 plates. Yields refer to chromatographically and spectroscopically pure compounds. <sup>1</sup>H NMR and <sup>13</sup>C NMR spectra were recorded on a Varian Inova-300 (300 and 75 MHz, respectively), Bruker Avance ARX-400 (400 and 100 MHz), and Bruker Avance DRX-500 (500 and 125 MHz). High- and low-resolution mass spectra were carried out by the Mass Spectroscopy Center at Purdue University. The purity of all test compounds was determined by HRMS and HPLC analysis. All test compounds showed ≥95% purity.

**3,3a,5,6,7,8a-Hexahydrofuro[2,3-b]benzofuran-4(2H)-one (5a).** Manganese(III) acetate (5.74 g, 21.4 mmol) was dissolved in 80.0 mL of glacial acetic acid at 60 °C under argon. To this mixture was added cyclohexane-1,3-dione (1 g, 8.92 mmol) and 2,3-dihydrofuran (1.35 mL, 17.8 mmol), and the reaction was stirred for 24 h. The reaction was diluted with water and extracted with dichloromethane (×4). The organic extracts were combined and washed with saturated aqueous sodium bicarbonate. The organic extracts were dried over Na<sub>2</sub>SO<sub>4</sub> and evaporated under reduced pressure. The residue was purified by column chromatography on silica gel using a hexane/ethyl acetate (1:3) solvent system to furnish the desired ketone (0.47 g, 30% yield). *R*<sub>f</sub> = 0.3 (50% hexanes/ethyl acetate); <sup>1</sup>H NMR (400 MHz, CDCl<sub>3</sub>) δ 6.22 (d, *J* = 5.9 Hz, 1H), 4.07 (t, *J* = 8.2 Hz, 1H), 3.70 (t, *J* = 7.7, 5.8 Hz, 1H), 3.65–3.62 (m, 1H), 2.55–2.37 (m, 2H), 2.32 (dd, *J* = 7.3, 5.8 Hz, 2H), 2.12–2.05 (m, 1H), 2.05–1.95 (m, 3H); <sup>13</sup>C NMR

(100 MHz, CDCl<sub>3</sub>) δ 195.2, 177.4, 113.6, 112.8, 67.8, 43.8, 36.6, 30.3, 23.6, 21.6.

**6,6-Dimethyl-3,3a,5,6,7,8a-decahydrofuro[2,3-b]benzofuran-4(2H)-one (5b).** The titled compound was obtained following the procedure outlined for compound 5a (42% yield). *R*<sub>f</sub> = 0.40 (50% hexanes/ethyl acetate); <sup>1</sup>H NMR (400 MHz, CDCl<sub>3</sub>) δ 6.18 (d, *J* = 5.8 Hz, 1H), 4.02 (t, *J* = 8.4 Hz, 1H), 3.65 (t, *J* = 7.7 Hz, 1H), 3.58–3.52 (m, 1H), 2.26 (d, *J* = 2.7 Hz, 2H), 2.14 (d, *J* = 6.5 Hz, 2H), 2.04–1.97 (m, 2H), 1.03 (s, 3H), 1.01 (s, 3H); <sup>13</sup>C NMR (100 MHz, CDCl<sub>3</sub>) δ 194.3, 176.1, 112.8, 112.0, 67.7, 50.8, 43.5, 37.4, 33.7, 30.2, 28.7, 28.0.

**2,3,3a,6,7,8a-Hexahydrofuro[2,3-b]benzofuran-4(5H)-one (5c).** The titled compound was obtained following the procedure outlined for compound 5d (77% yield). *R*<sub>f</sub> = 0.43 (50% ethyl acetate/hexanes); <sup>1</sup>H NMR (400 MHz, CDCl<sub>3</sub>) δ 5.92 (d, *J* = 7.6 Hz, 1H), 3.87–3.71 (m, 2H), 3.15–3.09 (m, 1H), 2.55–2.44 (m, 2H), 2.37–2.29 (m, 2H), 2.07–1.98 (m, 2H), 1.97–1.86 (m, 1H), 1.82–1.74 (m, 1H), 1.71–1.61 (m, 1H), 1.60–1.51 (m, 1H); <sup>13</sup>C NMR (100 MHz, CDCl<sub>3</sub>) δ 195.3, 176.3, 116.0, 106.6, 60.5, 36.5, 35.1, 23.6, 21.5, 20.3, 19.1.

**3,3a,7,8a-Tetrahydro-2H-furo[3',2':4,5]furo[2,3-c]pyran-4(5H)-one (5d).** To a solution of 2,3-dihydrofuran (6.0 mL) and diazo compound 11b (300 mg, 0.32 mmol, 1.0 eq) was added rhodium(II) diacetate (13.0 mg, 0.03 mmol, 1.5 mol %). The mixture was allowed to stir for 3 h. Upon completion, the reaction was concentrated under vacuum and purified by flash chromatography (15% ethyl acetate/hexanes) to give the desired tricyclic product as a colorless oil (260 mg, 67% yield). *R*<sub>f</sub> = 0.40 (40% ethyl acetate/hexanes); <sup>1</sup>H NMR (400 MHz, CDCl<sub>3</sub>) δ 6.33 (d, *J* = 5.8 Hz, 1H), 4.40 (q, *J* = 16.7 Hz, 2H), 4.10 (t, *J* = 8.2 Hz, 1H), 4.00 (s, 2H), 3.74 (t, *J* = 7.6 Hz, 1H), 3.66 (m, 1H), 2.13–1.98 (m, 2H); <sup>13</sup>C NMR (100 MHz, CDCl<sub>3</sub>) δ 191.0, 175.0, 114.6, 111.3, 71.0, 68.1, 62.1, 43.1, 29.9; LRMS-EI (*m/z*) 182 (*M*<sup>+</sup>), LRMS-CI (*m/z*) 183 (*M*<sup>+</sup> + H).

**2,3,3a,8a-Tetrahydro-5H-furo[2,3-b]thiopyrano[4,3-d]furan-4(7H)-one 6,6-dioxide (5e).** The titled compound was obtained following the procedure outlined for compound 5b (48% yield). *R*<sub>f</sub> = 0.38 (50% ethyl acetate/hexanes); <sup>1</sup>H NMR (400 MHz, CDCl<sub>3</sub>) δ 6.33 (d, *J* = 5.9 Hz, 1H), 4.16–4.07 (m, 2H), 3.95 (d, *J* = 1.6 Hz, 2H), 3.84–3.77 (m, 1H), 3.69–3.60 (m, 2H), 2.14–2.06 (m, 2H); <sup>13</sup>C NMR (100 MHz, CDCl<sub>3</sub>) δ 180.6, 166.2, 115.0, 113.9, 68.1, 60.1, 50.8, 44.3, 29.9.

**4-Diazo-2H-pyran-3,5(4H,6H)-dione (11b).** Ethyl 2-(2-oxopropoxy) acetate (15.0 g) was dissolved in THF (250 mL) and added dropwise (over 5 h) to a THF (1.0 L) solution of potassium *t*-butoxide (11.5 g, 103 mmol, 1.1 equiv) at 65 °C. Once the addition was complete, the reaction mixture was stirred for 15 min at 65 °C and then concentrated under vacuum to give a brown solid. Ethyl acetate was added to the solid, and 6 N HCl (20.0 mL) was added slowly while vigorously stirring the suspension. The organic layer was separated, dried over magnesium sulfate, and concentrated under vacuum (<20 °C). The crude mixture (~7.0 g, 61.3 mmol, 2.0 equiv) was dissolved in THF and cooled to 0 °C, and triethylamine (10.0 mL, 70.0 mmol, 2.30 equiv) and sulfonyl azide (6.0 g, 30.4 mmol, 1.0 equiv) were added sequentially. The reaction was allowed to stir for 4 h. Upon completion, the reaction was concentrated under vacuum and purified by flash chromatography (20% ethyl acetate/hexanes) to give the desired diazo compound as a light-yellow solid (3.0 g, 23% in two steps). Note that to remove trace amounts of the TsNH<sub>2</sub> byproduct, the diazo compound was recrystallized from diethyl ether. *R*<sub>f</sub> = 0.86 (50% ethyl acetate/hexanes); <sup>1</sup>H NMR (400 MHz, CDCl<sub>3</sub>) δ 4.27 (s, 4 H). <sup>13</sup>C NMR (100 MHz, CDCl<sub>3</sub>) δ 186.6, 71.9.

**4-Diazo-2H-thiopyran-3,5(4H,6H)-dione 1,1-Dioxide (11d).** In a dry flask, 2-chloro-1,3-dimethylimidazolium chloride (890 mg, 5.26 mmol) was dissolved in MeCN (9 mL), and sodium azide (342 mg, 5.23 mmol) was added at 0 °C and stirred for 30 min. A cooled solution of 10b (500 mg, 4.39 mmol) and triethylamine (1.22 mL, 8.88 mmol) in THF (18 mL) was cannulated to the mixture. The reaction was monitored by TLC until 10b was consumed, and the reaction was quenched with water and extracted three times with CH<sub>2</sub>Cl<sub>2</sub>. The organic layers were combined, dried over Na<sub>2</sub>SO<sub>4</sub>, and concentrated under vacuum, and the residue was purified by flash chromatography using (6:1) hexanes/ether to obtain 11c (290 mg, 68% yield) as an off-

white crystalline solid.  $^1\text{H NMR}$  (400 MHz,  $\text{CDCl}_3$ )  $\delta$  3.41 (s, 4H);  $^{13}\text{C NMR}$  (100 MHz,  $\text{CDCl}_3$ )  $\delta$  185.4, 35.7.

In a flask, diazo compound **11c** (740 mg, 4.74 mmol) was dissolved in a mixture of  $\text{H}_2\text{O}$  (5 mL) in MeOH (30 mL). To the solution was added oxone (5.00 g, 9.50 mmol), and the mixture was stirred for 3 h. Upon completion, the reaction was filtered on Celite, and the pad was washed with ether. Methanol and ether were removed under reduced pressure ( $<30^\circ\text{C}$ ), and the resulting aqueous mixture was extracted with dichloromethane three times. The combined extracts were combined, dried over  $\text{Na}_2\text{SO}_4$ , and concentrated ( $<30^\circ\text{C}$ ). The crude residue was purified by flash chromatography using 3:1 hexanes/ether to obtain **11d** (630 mg, 82% yield)  $R_f = 0.42$  ( $\text{SiO}_2$ , hexanes/EtOAc = 1/1);  $^1\text{H NMR}$  (400 MHz,  $\text{CDCl}_3$ )  $\delta$  4.20 (s, 4H);  $^{13}\text{C NMR}$  (100 MHz,  $\text{CDCl}_3$ )  $\delta$  176.6, 60.4.

**Decahydrofuro[2,3-*b*]benzofuran-4-ol (6a)**. To a solution of enone **5a** (44.0 mg, 2.22 mmol) in ethanol (15.0 mL) was added 10% Pd/C (44.0 mg). The resulting solution was then placed under 65 psi  $\text{H}_2$  gas overnight. Upon completion, the mixture was filtered through a plug of Celite. Evaporation of the solvent and purification of the residue on silica gel using ethyl acetate/hexanes (3:1) as the eluent furnished the corresponding compound as a colorless oil (0.23 g, 52% yield).  $R_f = 0.26$  (50% hexane/ethyl acetate);  $^1\text{H NMR}$  (400 MHz,  $\text{CDCl}_3$ )  $\delta$  5.66 (d,  $J = 4.9$  Hz, 1H), 4.39–4.43 (m, 1H), 3.92 (dd,  $J = 7.7, 6.1$  Hz, 2H), 3.18–3.11 (m, 1H), 3.02 (t,  $J = 12.0$  Hz, 1H), 2.44–2.29 (m, 2H), 2.11–1.79 (m, 4H), 1.75–1.60 (m, 2H);  $^{13}\text{C NMR}$  (100 MHz,  $\text{CDCl}_3$ )  $\delta$  211.4, 108.3, 77.3, 68.2, 51.9, 46.8, 40.8, 28.7, 27.8, 17.7.

To a cold solution ( $0^\circ\text{C}$ ) of the above ketone (230 mg, 1.25 mmol) in methanol (10 mL) was added  $\text{NaBH}_4$  (57 mg, 1.5 mmol), and the mixture was stirred for 1 h at  $0^\circ\text{C}$ . The reaction was quenched with saturated  $\text{NH}_4\text{Cl}$ , and the methanol was removed under vacuum. The aqueous layer was washed with ethyl acetate. The organic layers were combined, dried over  $\text{Na}_2\text{SO}_4$ , concentrated under reduced pressure, and purified by column chromatography using an ethyl acetate/hexane (1:1) solvent system to afford the corresponding alcohol (217 mg, 95% yield).  $R_f = 0.18$  (hexane/ethyl acetate 1:1);  $^1\text{H NMR}$  (500 MHz,  $\text{CDCl}_3$ )  $\delta$  5.69 (d,  $J = 5.3$  Hz, 1H), 4.24–4.17 (m, 1H), 3.97 (q,  $J = 7.4$  Hz, 1H), 3.89–3.78 (m, 2H), 3.01–2.94 (m, 1H), 2.20–2.10 (m, 1H), 2.00 (q,  $J = 4.5$  Hz, 1H), 1.95–1.85 (m, 2H), 1.81–1.70 (m, 2H), 1.69–1.55 (m, 2H), 1.52–1.45 (m, 1H), 1.37–1.28 (m, 1H);  $^{13}\text{C NMR}$  (100 MHz,  $\text{CDCl}_3$ )  $\delta$  100.9, 76.7, 65.2, 63.2, 43.9, 40.4, 31.4, 27.8, 21.4, 20.5, 15.6; LRMS-EI ( $m/z$ ) 185 (M + H).

**6,6-Dimethyloctahydrofuro[2,3-*b*]benzofuran-4(2H)-ol (6b)**. The target compound was obtained following the procedures outlined for compound **6a** (17% yield).  $R_f = 0.53$  (50% hexane/ethyl acetate);  $^1\text{H NMR}$  (400 MHz,  $\text{CDCl}_3$ )  $\delta$  5.61 (d,  $J = 5.3$  Hz, 1H), 4.66 (t,  $J = 6.0$  Hz, 1H), 3.92–3.85 (m, 2H), 3.20–3.05 (m, 2H), 2.25–2.22 (m, 1H), 2.22–2.09 (m, 1H), 2.03–1.95 (m, 1H), 1.81 (dd,  $J = 15.0, 4.7$  Hz, 2H), 1.77–1.68 (m, 1H), 1.02 (s, 3H), 0.95 (s, 3H);  $^{13}\text{C NMR}$  (100 MHz,  $\text{CDCl}_3$ )  $\delta$  209.0, 107.8, 79.9, 68.3, 57.1, 53.3, 42.9, 39.7, 35.4, 31.7, 31.0, 27.6.

The target alcohol was obtained following the procedure outlined for compound **6a** (step 2) (81% yield).  $R_f = 0.2$  (50% hexane/ethyl acetate);  $^1\text{H NMR}$  (400 MHz,  $\text{CDCl}_3$ )  $\delta$  5.70 (d,  $J = 5.2$  Hz, 1H), 4.39–4.22 (m, 2H), 4.13–4.06 (m, 1H), 3.93–3.83 (m, 1H), 2.96–2.81 (m, 2H), 2.22–2.12 (m, 2H), 2.08–2.00 (m, 1H), 1.70 (ddd,  $J = 13.2, 6.6, 1.9$  Hz, 1H), 1.59 (ddd,  $J = 13.0, 6.1, 2.0$  Hz, 1H), 1.42 (t,  $J = 12.5$  Hz, 1H), 1.30 (t,  $J = 12.5$  Hz, 1H), 0.97 (s, 3H), 0.86 (s, 3H);  $^{13}\text{C NMR}$  (100 MHz,  $\text{CDCl}_3$ )  $\delta$  109.9, 77.7, 68.6, 67.3, 45.2, 44.9, 44.0, 42.5, 32.8, 31.4, 27.8, 25.0; LRMS-CI ( $m/z$ ) 213.9 (M + H).

**(4*a*S,9*a*R)-Octahydro-2H-pyrano[2,3-*b*]benzofuran-5(3H)-ol (6c)**. The target compound was obtained following the procedure outlined for compound **6a** (62% yield).  $R_f = 0.45$  (50% ethyl acetate/hexanes);  $^1\text{H NMR}$  (400 MHz,  $\text{CDCl}_3$ )  $\delta$  5.03 (d,  $J = 3.7$  Hz, 1H), 4.46–4.20 (m, 1H), 3.86–3.81 (m, 1H), 3.55–3.49 (m, 1H), 2.82 (t,  $J = 8.5$  Hz, 1H), 2.46–2.41 (m, 1H), 2.39 (t,  $J = 6.5$  Hz, 1H), 2.34–2.29 (m, 1H), 2.24–2.11 (m, 1H), 1.96–1.71 (m, 4H), 1.69–1.61 (m, 1H), 1.52–1.42 (m, 1H), 1.42–1.32 (m, 1H);  $^{13}\text{C NMR}$  (100 MHz,  $\text{CDCl}_3$ )  $\delta$  212.0, 100.6, 76.2, 63.0, 50.9, 41.0, 40.4, 28.9, 22.1, 17.0.

The target alcohol was obtained following the procedure outlined for compound **6a** (step 2) (80% yield).  $R_f = 0.3$  (40% ethyl acetate/hexanes);  $^1\text{H NMR}$  (400 MHz,  $\text{CDCl}_3$ )  $\delta$  5.05 (d,  $J = 4.8$  Hz, 1H), 4.07–4.00 (m, 2H), 3.92–3.89 (m, 1H), 3.65–3.59 (m, 1H), 2.37–2.30 (m, 1H), 2.22–2.18 (m, 1H), 2.02–1.91 (m, 3H), 1.88–1.74 (m, 4H), 1.51–1.38 (m, 2H), 1.30–1.21 (m, 1H);  $^{13}\text{C NMR}$  (100 MHz,  $\text{CDCl}_3$ )  $\delta$  100.9, 77.3, 65.2, 63.2, 43.9, 40.2, 31.4, 27.8, 21.3, 20.5, 15.6.

**Octahydro-2H-furo[3',2':4,5]furo[2,3-*c*]pyran-4-ol (6d)**. Compound **5d** (260 mg, 1.4 mmol, 1.0 equiv) was treated with 10% Pd/C (35.0 mg) in methanol in the presence of hydrogen at 1 atm. The reaction was stirred for 12 h. Upon completion, the reaction was filtered through a plug of Celite, concentrated under vacuum, and purified by flash chromatography (gradient of 10–25% ethyl acetate/hexanes) to obtain the desired compound as a colorless oil (126 mg, 6:1 inseparable mixture of diastereomers, 48% yield).  $R_f = 0.3$  (50% ethyl acetate/hexanes);  $^1\text{H NMR}$  (400 MHz,  $\text{CDCl}_3$ )  $\delta$  5.72 (d,  $J = 5.1$  Hz, 1H, minor), 5.68 (d,  $J = 4.5$  Hz, 1H, major), 4.62 (dt,  $J = 6.6, 3.2$  Hz, 1H, minor), 4.39 (dt,  $J = 8.1, 3.3$  Hz, 1H, major), 4.14 (d,  $J = 16.7$  Hz, 1H, major), 4.07 (s, 1H, major), 4.04–4.00 (m, 2H, major), 3.97 (s, 2H, major), 3.95–3.87 (m, 2H, major), 3.70 (dd,  $J = 12.8, 3.2$  Hz, 1H, major), 3.43–3.38 (m, 1H, minor), 3.27–3.19 (m, 1H), 3.19–3.12 (m, 1H), 2.77 (dd,  $J = 6.5, 2.2$  Hz, 1H, minor), 2.24–2.20 (m, 1H, minor), 1.90 (q,  $J = 6.5$  Hz, 2H);  $^{13}\text{C NMR}$  (100 MHz,  $\text{CDCl}_3$ )  $\delta$  208.8 (major), 109.1 (minor), 108.8 (major), 75.2 (major), 75.0 (major), 73.9 (minor), 69.0 (major), 68.2 (major), 55.2 (minor), 49.6 (major), 46.9 (major), 44.6 (minor), 31.6 (minor), 27.2 (major); LRMS-CI ( $m/z$ ) 185.1 (M + H).

The ketone obtained above (120 mg, 0.65 mmol, 1.0 equiv) was dissolved in THF (5.0 mL) and cooled to  $-78^\circ\text{C}$ . L-Selectride (0.78 mL, 0.78 mmol, 1.2 equiv) was added dropwise, and the reaction was allowed to stir for 2 h. Upon completion, the reaction was quenched with saturated  $\text{NH}_4\text{Cl}$  (2.0 mL) and warmed to room temperature. The reaction mixture was diluted with ethyl acetate (5.0 mL) and extracted two more times. The organic layers were combined, washed with brine, and dried over  $\text{Mg}_2\text{SO}_4$ , and the residue was purified by flash chromatography to obtain desired compound **6d** (60 mg, 48% yield) as a colorless oil.  $R_f = 0.3$  (50% ethyl acetate/hexanes);  $^1\text{H NMR}$  (400 MHz,  $\text{CDCl}_3$ )  $\delta$  5.72 (d,  $J = 5.2$  Hz, 1H), 4.16 (d,  $J = 13.4$  Hz, 1H), 3.91 (s, 1H), 3.92–3.84 (m, 2H), 3.83–3.78 (m, 1H), 3.65–3.55 (m, 1H), 3.53 (d,  $J = 13.3$  Hz, 1H), 3.32 (d,  $J = 11.8$  Hz, 1H), 3.07–3.65 (q,  $J = 5.2$  Hz, 1H), 2.54 (d,  $J = 11.7$  Hz, 1H), 2.21–2.15 (m, 1H), 2.06 (t,  $J = 4.4$  Hz, 1H), 1.69–1.63 (m, 1H);  $^{13}\text{C NMR}$  (100 MHz,  $\text{CDCl}_3$ )  $\delta$  109.5, 74.1, 70.5, 68.3, 67.2, 65.3, 46.8, 46.0, 30.4.

**4-Hydroxyoctahydro-5H-furo[2,3-*b*]thiopyrano[4,3-*d*]furan 6,6-dioxide (6e)**. The target compound was obtained following the procedure outlined for compound **6d** (28% yield, 2 steps).  $R_f = 0.1$  (50% ethyl acetate/hexanes);  $^1\text{H NMR}$  (400 MHz,  $\text{CDCl}_3$ )  $\delta$  5.73 (d,  $J = 5.5$  Hz, 1H), 4.52–4.39 (m, 1H), 4.15–4.05 (m, 2H), 3.92–3.83 (m, 1H), 3.68 (dt,  $J = 12.9, 3.7$  Hz, 1H), 3.37 (dt,  $J = 14.6, 3.2$  Hz, 1H), 3.24–3.18 (m, 3H), 3.08–3.02 (m, 1H), 2.01–1.95 (m, 1H), 1.73 (dd,  $J = 12.8, 4.7$  Hz, 1H), 1.48 (td,  $J = 10.6, 2.1$  Hz, 1H);  $^{13}\text{C NMR}$  (100 MHz,  $\text{CDCl}_3$ )  $\delta$  109.0, 70.4, 67.1, 62.7, 57.5, 56.4, 52.3, 43.1, 30.1.

**(S)-Alcohol (8a)**. Alcohol (**6a**) (20.0 mg, 0.11 mmol) was dissolved in THF (1.0 mL) under argon. Lipase Amano PS-30 (25.0 mg) and vinyl acetate (0.18 mL, 1.91 mmol) were subsequently added at room temperature. The reaction was stirred until completion (50:50 by  $^1\text{H NMR}$ ), filtered through a plug of Celite, and concentrated under reduced pressure. The residue was purified by column chromatography on silica gel using ethyl acetate/hexanes (1:2) to yield the corresponding alcohol and acetate. (S)-alcohol **8a** (9 mg, 45% yield).  $R_f = 0.13$  (50% ethyl acetate/hexanes);  $[\alpha]_{\text{D}}^{23} +9.6$  (c 1.0,  $\text{CHCl}_3$ ). (R)-acetate **7a** (11 mg, 45% yield).  $R_f = 0.40$  (50% ethyl acetate/hexanes);  $[\alpha]_{\text{D}}^{23} -1.69$  (c 1.0,  $\text{CHCl}_3$ );  $^1\text{H NMR}$  (400 MHz,  $\text{CDCl}_3$ )  $\delta$  5.67 (d,  $J = 5.3$  Hz, 1H), 5.10–5.06 (m, 1H), 4.22 (q,  $J = 5.1$  Hz, 1H), 3.93–3.80 (m, 3H), 2.77–2.68 (m, 1H), 2.21 (q,  $J = 5.1$  Hz, 1H), 2.14–2.06 (m, 1H), 2.05 (s, 3H), 1.75–1.60 (m, 4H), 1.57–1.46 (m, 1H), 1.29–1.18 (m, 1H);  $^{13}\text{C NMR}$  (100 MHz,  $\text{CDCl}_3$ )  $\delta$  170.5, 108.9, 76.1, 70.2, 67.3, 46.3, 44.9, 31.3, 27.6, 27.5, 21.2, 15.7; LRMS-CI ( $m/z$ ) 229.1 (M + H).

(*R*)-Alcohol (**9a**). The titled compound was obtained from compound **7a** following the procedure for **9b** (89% yield).  $R_f = 0.13$  (50% ethyl acetate/hexanes);  $[\alpha]_D^{23} -9.7$  (c 1.0, CHCl<sub>3</sub>).

(*R*)-Alcohol (**8b**). To a solution of racemic alcohol **6d** (60.0 mg, 0.32 mmol, 1.0 equiv) in THF (10 mL) was added vinyl acetate (0.60 mL, 6.44 mmol, 20.0 equiv) and lipase PS-30 immobilized on Celite (120 mg total). The reaction was stirred for 20 h at 23 °C and monitored by NMR (1:1 mixture of alcohol and acetate after 20 h). Upon completion, the reaction was filtered through a plug of Celite, concentrated under vacuum, and purified by flash chromatography. (*R*)-alcohol **8b** was obtained as a colorless oil (28 mg, 47% yield).  $R_f = 0.24$  (80% ethyl acetate/hexanes);  $[\alpha]_D^{23} +12.1$  (c 0.8, CHCl<sub>3</sub>).

(*S*)-Acetate (**7b**). (35 mg, 48% yield, white solid).  $R_f = 0.32$  (80% ethyl acetate/hexanes);  $[\alpha]_D^{23} -27.3$  (c 1.2, CHCl<sub>3</sub>); <sup>1</sup>H NMR (400 MHz, CDCl<sub>3</sub>)  $\delta$  5.77 (d,  $J = 5.0$  Hz, 1H), 5.0 (d,  $J = 4.9$  Hz, 1H), 4.17 (d,  $J = 13.1$  Hz, 1H), 4.07 (dt,  $J = 4.7, 2.3$  Hz, 1H), 3.97–3.88 (m, 2H), 3.84 (d,  $J = 13.2$  Hz, 1H), 3.58 (d,  $J = 13.3$  Hz, 1H), 3.41 (d,  $J = 12.8$  Hz, 1H), 2.76–2.72 (m, 1H), 2.36 (t,  $J = 4.9$  Hz, 1H), 2.24–2.18 (m, 1H), 2.13 (s, 3H), 1.72–1.67 (m, 1H); <sup>13</sup>C NMR (100 MHz, CDCl<sub>3</sub>)  $\delta$  170.7, 109.5, 73.2, 67.9, 67.7, 67.3, 66.7, 45.6, 44.3, 30.5, 21.2. (*S*)-Alcohol **9b**: To a cold (0 °C) methanol solution of (*S*)-acetate **7b** was added a 1.0 M solution of NaOMe/MeOH (1.0 mL). The solution was stirred for 15 min and quenched with saturated NH<sub>4</sub>Cl. The reaction was concentrated under vacuum to remove the methanol and extracted with ethyl acetate. The organic layer was dried over Na<sub>2</sub>SO<sub>4</sub>, concentrated, and chromatographed (70% ethyl acetate/hexanes) to give the desired alcohol as a colorless oil (20 mg, 71% yield).  $[\alpha]_D^{23} -16.2$  (c 1.0, CHCl<sub>3</sub>).

(*S*)-Alcohol (**8c**) and (*R*)-Acetate (**7c**). The titled compound was obtained by enzymatic resolution of alcohol **6c** using the procedure described for (*R*)-alcohol **8b** and (*S*)-acetate **7b**. (*S*)-Alcohol **8c** (38% yield).  $[\alpha]_D^{23} -4.33$  (c 1.1, CHCl<sub>3</sub>). (*R*)-Acetate **7c** (39% yield).  $[\alpha]_D^{23} +7.04$  (c 1.4, CHCl<sub>3</sub>).

(3*aR*,3*bR*,4*S*,7*aR*,8*aS*)-Decahydrofuro[2,3-*b*]benzofuran-4-yl (4-Nitrophenyl) Carbonate (**14a**). To a solution of alcohol **8a** (7.0 mg, 0.04 mmol) in dichloromethane (1.0 mL) under argon atmosphere was added 4-nitrophenyl chloroformate (11.0 mg, 0.06 mmol), and the solution was cooled to 0 °C followed by the addition of pyridine (12.2  $\mu$ L, 0.15 mmol). The reaction was warmed to room temperature and stirred for 3 h (70% yield).  $R_f = 0.63$  (50% hexanes/ethyl acetate);  $[\alpha]_D^{23} +11.2$  (c 1.0, CHCl<sub>3</sub>); <sup>1</sup>H NMR (300 MHz, CDCl<sub>3</sub>)  $\delta$  8.29 (d,  $J = 9.2$  Hz, 2H), 7.39 (d,  $J = 9.2$  Hz, 2H), 5.78 (d,  $J = 5.2$  Hz, 1H), 5.11–5.03 (m, 1H), 4.29 (dd,  $J = 4.9, 9.9$  Hz, 1H), 4.00–3.85 (m, 2H), 2.95–2.83 (m, 1H), 2.35 (dd,  $J = 5.0, 9.6$  Hz, 1H), 2.26–2.11 (m, 1H), 1.98–1.62 (m, 6H), 1.37–1.28 (m, 1H); <sup>13</sup>C NMR (100 MHz, CDCl<sub>3</sub>)  $\delta$  155.5, 152.1, 145.3, 130.6, 123.7, 108.9, 75.6, 71.7, 67.6, 46.7, 45.4, 31.3, 27.9, 27.2, 15.6; LRMS-APCI ( $m/z$ ) 350.2 (M + H)<sup>+</sup>.

(3*aS*,3*bS*,4*R*,7*aS*,8*aR*)-Decahydrofuro[2,3-*b*]benzofuran-4-yl (4-Nitrophenyl) Carbonate (**14b**). The titled compound was obtained following the procedure outlined for compound **14a** (84% yield).  $R_f = 0.60$  (50% ethyl acetate/hexanes);  $[\alpha]_D^{23} -11.4$  (c 1.0, CHCl<sub>3</sub>).

6,6-Dimethyldecahydrofuro[2,3-*b*]benzofuran-4-yl (4-Nitrophenyl) Carbonate (**14c**). The titled compound was obtained following the procedure outlined above compound **14a** (97% yield).  $R_f = 0.68$  (50% ethyl acetate/hexanes); <sup>1</sup>H NMR (400 MHz, CDCl<sub>3</sub>)  $\delta$  8.29 (d,  $J = 9.2$  Hz, 2H), 7.37 (d,  $J = 9.2$  Hz, 2H), 5.77 (d,  $J = 5.3$  Hz, 1H), 5.21 (dt,  $J = 11.4, 5.5$  Hz, 1H), 4.50–4.37 (m, 1H), 3.97 (dd,  $J = 7.4, 6.4$  Hz, 1H), 3.90–3.86 (m, 1H), 3.01–2.98 (m, 1H), 2.62–2.59 (m, 1H), 2.08–2.04 (m, 1H), 1.97–1.86 (m, 1H), 1.79–1.69 (m, 2H), 1.67–1.55 (m, 1H), 1.22–1.12 (m, 1H), 1.03 (s, 3H), 0.93 (s, 3H); <sup>13</sup>C NMR (100 MHz, CDCl<sub>3</sub>)  $\delta$  155.4, 151.9, 145.4, 125.3, 121.7, 108.4, 76.0, 66.5, 44.6, 42.8, 40.6, 38.3, 32.4, 32.2, 30.9, 25.0; LRMS-APCI ( $m/z$ ) 378.1 (M + H)<sup>+</sup>.

(4*aR*,4*bR*,5*S*,8*aR*,9*aS*)-Decahydro-2*H*-pyrano[2,3-*b*]benzofuran-5-yl (4-Nitrophenyl) Carbonate (**14e**). The titled compound was obtained following the procedure outlined above compound **14a** (95% yield).  $R_f = 0.23$  (30% ethyl acetate/hexanes); <sup>1</sup>H NMR (400 MHz, CHCl<sub>3</sub>)  $\delta$  8.28 (d,  $J = 9.2$  Hz, 2H), 7.38 (d,  $J = 8.8$  Hz, 2H), 5.30 (d,  $J = 3.9$  Hz, 1H), 5.07–5.01 (m, 1H), 4.23–4.16 (m, 1H), 3.84 (td,  $J =$

11.3, 3.0 Hz, 1H), 3.72 (ddt,  $J = 11.0, 4.2, 2.0$  Hz, 1H), 3.04 (q,  $J = 8.2$  Hz, 1H), 2.18–2.10 (m, 2H), 2.06–2.02 (m, 2H), 1.94–1.82 (m, 2H), 1.75–1.54 (m, 4H), 1.37–1.24 (m, 1H); <sup>13</sup>C NMR (100 MHz, CDCl<sub>3</sub>)  $\delta$  155.4, 151.9, 145.4, 125.3, 121.8, 101.1, 78.3, 74.6, 61.1, 41.1, 37.1, 30.8, 28.2, 23.9, 23.3, 19.5

4-Nitrophenyl ((3*aR*,3*bR*,4*R*,7*aS*,8*aS*)-Octahydro-5*H*-furo[3',2':4,5]furo[2,3-*c*]pyran-4-yl) Carbonate (**14f**). The titled compound was obtained following the procedure outlined for compound **14a** (72% yield).  $R_f = 0.14$  (60% ethyl acetate/hexanes);  $[\alpha]_D^{23} +39.6$  (c 1.0, CHCl<sub>3</sub>); <sup>1</sup>H NMR (400 MHz, CDCl<sub>3</sub>)  $\delta$  8.27 (d,  $J = 8.9$  Hz, 2H), 7.40 (d,  $J = 9.0$  Hz, 2H), 5.87 (d,  $J = 5.0$  Hz, 1H), 4.89 (dt,  $J = 4.9, 2.2$  Hz, 1H), 4.25 (d,  $J = 13.1$  Hz, 1H), 4.16–4.12 (m, 2H), 3.97–4.01 (m, 1H), 3.88–3.93 (m, 1H), 3.64 (dd,  $J = 13.2, 2.4$  Hz, 1H), 3.49 (dd,  $J = 13.1, 1.0$  Hz, 1H), 2.92 (dt,  $J = 10.2, 5.0$  Hz, 1H), 2.46 (t,  $J = 4.9$  Hz, 1H), 2.21–2.31 (m, 1H), 1.71–1.77 (m, 1H); <sup>13</sup>C NMR (100 MHz, CDCl<sub>3</sub>)  $\delta$  155.2, 152.2, 145.3, 125.3, 121.6, 109.5, 73.1, 72.5, 68.0, 67.4, 67.0, 45.8, 44.5, 30.6; LRMS-CI ( $m/z$ ) 374.3 (M + Na).

4-Nitrophenyl ((3*aS*,3*bS*,4*S*,7*aR*,8*aR*)-Octahydro-5*H*-furo[3',2':4,5]furo[2,3-*c*]pyran-4-yl) Carbonate (**14g**). The titled compound was obtained following the procedure outlined above compound **14a** (97% yield).  $R_f = 0.14$  (60% ethyl acetate/hexanes);  $[\alpha]_D^{23} -41.4$  (c 0.95, CHCl<sub>3</sub>).

6,6-Dioxidoctahydro-5*H*-furo[2,3-*b*]thiopyrano[4,3-*d*]furan-4-yl (4-Nitrophenyl) Carbonate (**14h**). The titled compound was obtained following the procedure outlined above compound **14a** (52% yield).  $R_f = 0.28$  (50% ethyl acetate/hexanes); <sup>1</sup>H NMR (400 MHz, CDCl<sub>3</sub>)  $\delta$  8.29 (d,  $J = 9.2$  Hz, 2H), 7.42 (d,  $J = 9.2$  Hz, 2H), 5.79 (d,  $J = 5.5$  Hz, 1H), 5.33–5.31 (m, 1H), 4.25 (td,  $J = 11.6, 3.8$  Hz, 1H), 4.14–4.11 (m, 1H), 3.94–3.88 (m, 1H), 3.82–3.71 (m, 2H), 3.34–3.23 (m, 2H), 3.17–3.10 (m, 1H), 2.97–2.91 (m, 1H), 2.07–1.97 (m, 1H), 1.84–1.72 (m, 1H); <sup>13</sup>C NMR (100 MHz, CDCl<sub>3</sub>)  $\delta$  154.9, 151.6, 145.7, 125.4, 121.7, 108.8, 70.7, 69.0, 67.0, 57.7, 53.5, 50.2, 43.0, 30.2.

(3*aS*,3*bR*,4*S*,7*aR*,8*aS*)-Decahydrofuro[2,3-*b*]benzofuran-4-yl ((2*S*,3*R*)-3-Hydroxy-4-(*N*-isobutyl-4-methoxyphenylsulfonamido)-1-phenylbutan-2-yl)carbamate (**16a**). To a solution of activated alcohol **14a** (1.0 equiv) and isostere **15** (1.0 equiv) in acetonitrile was added triethylamine (5.0 equiv). The reaction was allowed to stir until the consumption of the activated alcohol. The reaction mixture was concentrated under vacuum and purified by flash column chromatography to provide inhibitor **16a** (63% yield).  $R_f = 0.3$  (50% hexanes/ethyl acetate);  $[\alpha]_D^{23} +7.8$  (c 1.0, CHCl<sub>3</sub>); <sup>1</sup>H NMR (400 MHz, CDCl<sub>3</sub>)  $\delta$  7.73 (d,  $J = 8.7$  Hz, 2H), 7.29 (d,  $J = 7.4$  Hz, 3H), 7.21 (dd,  $J = 12.4, 6.9$  Hz, 2H), 6.99 (d,  $J = 8.8$  Hz, 2H), 5.41 (d,  $J = 5.1$  Hz, 1H), 4.96–4.85 (m, 1H), 4.81 (d,  $J = 8.9$  Hz, 1H), 4.23–4.08 (m, 1H), 3.88 (s, 3H), 3.87–3.72 (m, 4H), 3.17 (dd,  $J = 15.3, 8.4$  Hz, 1H), 3.11–2.99 (m, 2H), 2.99–2.92 (m, 1H), 2.79 (td,  $J = 14.4, 13.8, 8.2$  Hz, 2H), 2.36–2.34 (m, 1H), 2.06 (d,  $J = 5.1$  Hz, 1H), 1.99–1.87 (m, 1H), 1.83 (dd,  $J = 13.8, 7.0$  Hz, 1H), 1.79–1.71 (m, 1H), 1.68–1.53 (m, 3H), 1.48–1.36 (m, 2H), 1.22 (bs, 2H), 0.93 (d,  $J = 6.6$  Hz, 3H), 0.88 (d,  $J = 6.5$  Hz, 3H); <sup>13</sup>C NMR (100 MHz, CDCl<sub>3</sub>)  $\delta$  163.0, 156.0, 137.6, 129.7, 129.4, 129.3, 128.4, 126.4, 114.3, 108.9, 75.7, 73.1, 70.1, 67.5, 58.7, 55.5, 54.7, 53.7, 46.6, 44.8, 35.6, 31.1, 29.6, 28.0, 27.3, 27.1, 20.1, 19.8, 15.2; LRMS-ESI ( $m/z$ ) 617.8 [M + H]<sup>+</sup>; HRMS-ESI ( $m/z$ ) [M + H]<sup>+</sup> calcd for (C<sub>32</sub>H<sub>44</sub>N<sub>2</sub>O<sub>8</sub>S), 617.2896; found, 617.2892.

(3*aS*,3*bS*,4*R*,7*aS*,8*aR*)-Decahydrofuro[2,3-*b*]benzofuran-4-yl ((2*S*,3*R*)-3-Hydroxy-4-(*N*-isobutyl-4-methoxyphenylsulfonamido)-1-phenylbutan-2-yl)carbamate (**16b**). The indicated inhibitor was obtained following the general procedure outlined above for inhibitor **16a** (52% yield).  $R_f = 0.31$  (50% hexanes/ethyl acetate);  $[\alpha]_D^{23} +8.0$  (c 1.0, CHCl<sub>3</sub>); <sup>1</sup>H NMR (400 MHz, CDCl<sub>3</sub>)  $\delta$  7.72 (d,  $J = 8.5$  Hz, 2H), 7.39–7.13 (m, 5H), 7.07–6.88 (m, 2H), 5.57 (d,  $J = 4.7$  Hz, 1H), 4.92 (d,  $J = 8.4$  Hz, 1H), 4.86 (s, 1H), 4.18 (s, 1H), 3.98–3.70 (m, 7H), 3.22–2.90 (m, 4H), 2.90–2.72 (m, 2H), 2.66 (s, 1H), 2.13 (s, 1H), 2.08–2.01 (m, 1H), 1.82 (dt,  $J = 15.5, 7.8$  Hz, 3H), 1.59 (d,  $J = 9.4$  Hz, 3H), 1.49–1.41 (m, 1H), 1.36–1.39 (m, 1H), 1.22–1.14 (m, 1H), 0.92 (d,  $J = 6.5$  Hz, 3H), 0.88 (d,  $J = 6.7$  Hz, 3H); <sup>13</sup>C NMR (100 MHz, CDCl<sub>3</sub>)  $\delta$  163.0, 156.1, 137.7, 129.8, 129.4, 129.3, 128.4, 126.4, 114.3, 108.9, 75.8, 72.6, 70.4, 67.4, 58.7, 55.5, 55.2, 53.6, 46.7,

45.1, 35.4, 31.2, 27.8, 27.3, 27.2, 20.1, 19.8, 15.2; LRMS-ESI ( $m/z$ ) 617.80 ( $M + H$ )<sup>+</sup>. HRMS-ESI ( $m/z$ ) [ $M + Na$ ]<sup>+</sup> calcd for (C<sub>33</sub>H<sub>44</sub>N<sub>2</sub>O<sub>8</sub>SNa), 639.2716; found, 639.2719.

(3*aS*,3*bR*,4*S*,7*aR*,8*aS*)-6,6-Dimethyldecahydrofuro[2,3-*b*]benzofuran-4-yl ((2*S*,3*R*)-3-Hydroxy-4-(*N*-isobutyl-4-methoxyphenylsulfonamido)-1-phenylbutan-2-yl)carbamate (**16c**). The indicated inhibitor was obtained following the general procedure outlined above for inhibitor **16a**. The product was obtained as a mixture of diastereomers (**16c/16d**) (61% yield, **16c/16d**).  $R_f = 0.33$ , (50% hexanes/ethyl acetate). **16c/16d** were separated by HPLC with column YMC-Pack-ODS-A (250 × 10 mm) and a solvent/flow rate of 2.5 mL/min (CH<sub>3</sub>CN/H<sub>2</sub>O, 65:35). Retention time: **16c** = 18.31 min and **16d** = 18.99 min. For **16c**: [ $\alpha$ ]<sub>D</sub><sup>23</sup> -19.0 (c 0.6, CHCl<sub>3</sub>); <sup>1</sup>H NMR (400 MHz, CDCl<sub>3</sub>)  $\delta$  7.73 (d,  $J = 8.9$  Hz, 2H), 7.28 (s, 2H), 7.25–7.18 (m, 3H), 6.99 (d,  $J = 8.9$  Hz, 2H), 5.57 (d,  $J = 5.0$  Hz, 1H), 5.01–4.94 (m, 1H), 4.82 (d,  $J = 8.9$  Hz, 1H), 4.26–4.15 (m, 1H), 4.05 (q,  $J = 8.1$  Hz, 2H), 3.94 (s, 1H), 3.88 (s, 4H), 3.83 (s, 1H), 3.24–3.10 (m, 2H), 3.01–2.95 (m, 1H), 2.87 (d,  $J = 8.3$  Hz, 2H), 2.80 (d,  $J = 13.2$  Hz, 2H), 2.15–2.05 (m, 1H), 2.03–1.90 (m, 2H), 1.89–1.80 (m, 2H), 1.75–1.55 (m, 3H) 0.97–0.94 (m, 6H), 0.90–0.86 (m, 6H); <sup>13</sup>C NMR (125 MHz, CDCl<sub>3</sub>)  $\delta$  163.0, 155.7, 137.7, 129.6, 129.4, 129.2, 128.4, 127.7, 126.5, 114.3, 113.8, 109.7, 73.1, 71.0, 68.4, 58.8, 55.6, 54.7, 53.7, 44.6, 42.4, 41.3, 40.7, 35.6, 32.6, 31.2, 27.7, 27.2, 24.6, 20.1, 19.8. HRMS-ESI ( $m/z$ ) [ $M + H$ ]<sup>+</sup> calcd for (C<sub>34</sub>H<sub>48</sub>N<sub>2</sub>O<sub>8</sub>S), 645.3209; found, 645.3210.

3*aS*,3*bS*,4*R*,7*aS*,8*aR*)-6,6-Dimethyldecahydrofuro[2,3-*b*]benzofuran-4-yl ((2*S*,3*R*)-3-Hydroxy-4-(*N*-isobutyl-4-methoxyphenylsulfonamido)-1-phenylbutan-2-yl)carbamate (**16d**). [ $\alpha$ ]<sub>D</sub><sup>23</sup> +21.5 (c 0.6, CHCl<sub>3</sub>); <sup>1</sup>H NMR (500 MHz, CDCl<sub>3</sub>)  $\delta$  7.70 (d,  $J = 8.3$  Hz, 2H), 7.43–7.13 (m, 5H), 6.98 (d,  $J = 8.6$  Hz, 2H), 5.69 (s, 1H), 5.10–4.98 (m, 1H), 4.93 (d,  $J = 8.3$  Hz, 1H), 4.27 (s, 1H), 4.09 (d,  $J = 6.5$  Hz, 1H), 3.87 (s, 6H), 3.64 (s, 1H), 3.13–3.08 (m, 1H), 3.02 (d,  $J = 14.3$  Hz, 2H), 2.96–2.91 (m, 2H), 2.79 (dd,  $J = 13.4$ , 6.7 Hz, 1H), 2.68 (s, 1H), 2.08–2.05 (m, 1H), 1.90–1.54 (m, 1H), 1.86–1.80 (m, 1H), 1.75–1.71 (m, 1H), 1.64–1.61 (s, 1H), 1.55–1.51 (s, 1H), 0.95 (s, 3H), 0.91–0.86 (m, 9H); <sup>13</sup>C NMR (125 MHz, CDCl<sub>3</sub>)  $\delta$  163.1, 156.13, 137.7, 129.7, 129.4, 128.5, 126.5, 114.3, 113.9, 109.8, 72.6, 71.1, 68.5, 58.8, 55.6, 55.2, 53.6, 45.3, 42.4, 41.3, 35.1, 32.7, 31.9, 31.3, 27.8, 27.3, 24.8, 22.7, 20.1, 19.9; HRMS-ESI ( $m/z$ ) [ $M + Na$ ]<sup>+</sup> calcd for (C<sub>34</sub>H<sub>48</sub>N<sub>2</sub>O<sub>8</sub>SNa), 667.3209; found, 667.3040.

(4*aR*,4*bR*,5*S*,8*aR*,9*aS*)-Decahydro-2*H*-pyrano[2,3-*b*]benzofuran-5-yl ((2*S*,3*R*)-3-Hydroxy-4-(*N*-isobutyl-4-methoxyphenylsulfonamido)-1-phenylbutan-2-yl)carbamate (**16e**). The indicated inhibitor was obtained following the general procedure outlined above for inhibitor **16a** (80% yield).  $R_f = 0.31$  (ethyl acetate/hexanes); <sup>1</sup>H NMR (400 MHz, CDCl<sub>3</sub>)  $\delta$  7.70 (d,  $J = 8.9$  Hz, 2H), 7.32–7.19 (m, 5H), 6.98 (d,  $J = 8.9$  Hz, 2H), 5.12 (d,  $J = 3.9$  Hz, 1H), 5.01 (dd,  $J = 18.6$ , 4.5 Hz, 1H), 4.96–4.86 (m, 1H), 4.86–4.72 (m, 1H), 4.41–4.30 (m, 1H), 3.87 (s, 3H), 3.86–3.73 (m, 2H), 3.67 (d,  $J = 12.2$  Hz, 1H), 3.41 (t,  $J = 10.7$  Hz, 1H), 3.18–3.07 (m, 1H), 3.07–2.99 (m, 2H), 2.99–2.70 (m, 2H), 2.58 (dd,  $J = 15.0$ , 7.4 Hz, 1H), 2.06 (ddd,  $J = 16.0$ , 10.5, 6.4 Hz, 1H), 1.88–1.68 (m, 2H), 1.53 (s, 4H), 1.53–1.37 (m, 4H), 1.35–1.16 (m, 2H), 0.91 (d,  $J = 6.7$  Hz, 3H), 0.87 (d,  $J = 6.7$  Hz, 3H); <sup>13</sup>C NMR (100 MHz, CDCl<sub>3</sub>)  $\delta$  163.0, 155.8, 137.6, 129.5, 129.4, 128.4, 126.5, 114.3, 100.9, 74.5, 73.0, 72.6, 61.0, 58.7, 55.5, 54.7, 53.7, 41.2, 36.6, 35.4, 30.9, 29.6, 28.6, 27.2, 23.8, 23.3, 21.9, 20.1, 19.8; HRMS-ESI ( $m/z$ ) [ $M + H$ ]<sup>+</sup> calcd for (C<sub>33</sub>H<sub>46</sub>N<sub>2</sub>O<sub>8</sub>S), 631.3053; found, 631.3047.

(3*aS*,3*bR*,4*R*,7*aS*,8*aS*)-Octahydro-2*H*-furo[3',2':4,5]furo[2,3-*c*]pyran-4-yl ((2*S*,3*R*)-3-Hydroxy-4-(*N*-isobutyl-4-methoxyphenylsulfonamido)-1-phenylbutan-2-yl)carbamate (**16f**). The indicated inhibitor was obtained following the general procedure outlined above for inhibitor **16a** (82% yield).  $R_f = 0.42$  (80% ethyl acetate/hexanes); [ $\alpha$ ]<sub>D</sub><sup>23</sup> +12.8 (c 1.0, CHCl<sub>3</sub>); <sup>1</sup>H NMR (400 MHz, *d*-MeOH)  $\delta$  7.79 (d,  $J = 8.8$  Hz, 2H), 7.29–7.26 (m, 4H), 7.22–7.16 (m, 1H), 7.11 (d,  $J = 8.8$  Hz, 2H), 5.51 (d,  $J = 4.8$  Hz, 1H), 4.67 (d,  $J = 5.2$  Hz, 1H), 4.05 (d,  $J = 8.0$  Hz, 1H), 3.98 (s, 1H), 3.89 (s, 4H), 3.81–3.84 (m, 3H), 3.71 (d,  $J = 12.0$  Hz, 1H), 3.61 (dd,  $J = 13.2$ , 2.0 Hz, 1H), 3.47–3.39 (m, 2H), 3.26–3.23 (m, 1H), 3.11 (dd,  $J = 13.5$ , 8.4 Hz, 1H), 2.95 (dd,  $J = 14.8$ , 8.1 Hz, 1H), 2.86 (dd,  $J = 13.5$ , 6.6 Hz, 1H), 2.63–2.46 (dd,  $J = 13.6$ , 2.8 Hz, 1H), 2.32 (t,  $J = 4.9$  Hz, 1H), 2.16–2.09 (m,

1H), 2.08–2.04 (m, 2H), 1.73–1.59 (m, 2H), 0.97 (d,  $J = 6.4$  Hz, 3H), 0.90 (t,  $J = 7.0$  Hz, 3H); <sup>13</sup>C NMR (100 MHz, *d*-MeOH)  $\delta$  164.6, 158.0, 140.2, 131.9, 130.7, 130.6, 129.3, 127.1, 115.4, 110.8, 75.0, 74.4, 69.2, 69.1, 68.2, 68.0, 59.0, 57.2, 56.2, 54.1, 46.8, 45.6, 37.3, 31.2, 28.0, 20.5; HRMS-ESI ( $m/z$ ) [ $M + H$ ]<sup>+</sup> calcd for (C<sub>31</sub>H<sub>42</sub>N<sub>2</sub>O<sub>9</sub>S), 619.2689; found, 619.2679.

(3*aS*,3*bS*,4*S*,7*aR*,8*aR*)-Octahydro-2*H*-furo[3',2':4,5]furo[2,3-*c*]pyran-4-yl ((2*S*,3*R*)-3-Hydroxy-4-(*N*-isobutyl-4-methoxyphenylsulfonamido)-1-phenylbutan-2-yl)carbamate (**16g**). The indicated inhibitor was obtained following the general procedure outlined above for inhibitor **16a** (70% yield).  $R_f = 0.27$  (80% ethyl acetate/hexanes); [ $\alpha$ ]<sub>D</sub><sup>23</sup> -11.5 (c 1.7, CHCl<sub>3</sub>); <sup>1</sup>H NMR (400 MHz, *d*-MeOH)  $\delta$  7.79 (d,  $J = 8.8$  Hz, 2H), 7.30–7.24 (m, 4H), 7.21–7.17 (m, 1H), 7.11 (d,  $J = 8.8$  Hz, 2H), 5.72 (d,  $J = 5.0$  Hz, 1H), 4.70 (d,  $J = 5.2$  Hz, 1H), 4.14–3.97 (m, 2H), 3.90 (s, 4H), 3.76–3.81 (m, 2H), 3.70 (dd,  $J = 10.7$ , 7.1 Hz, 1H), 3.61 (dd,  $J = 13.4$ , 2.4 Hz, 1H), 3.57–3.43 (m, 2H), 3.26–3.13 (m, 1H), 3.10–2.98 (m, 2H), 2.92 (dd,  $J = 13.6$ , 7.1 Hz, 1H), 2.73 (dt,  $J = 10.0$ , 4.8 Hz, 1H), 2.65 (dd,  $J = 13.7$ , 10.9 Hz, 1H), 2.43 (t,  $J = 4.9$  Hz, 1H), 2.25–2.10 (m, 1H), 2.06–1.97 (m, 2H), 1.86–1.69 (m, 1H), 1.05–0.83 (m, 6H); <sup>13</sup>C NMR (100 MHz, *d*-MeOH)  $\delta$  164.5, 158.0, 140.2, 132.3, 130.6, 130.5, 129.2, 127.2, 115.4, 110.8, 79.5, 75.0, 74.0, 69.0, 68.3, 68.1, 58.6, 57.6, 56.2, 53.8, 47.1, 45.5, 37.1, 31.3, 28.0, 20.5; HRMS-ESI ( $m/z$ ) [ $M + Na$ ]<sup>+</sup> calcd for (C<sub>31</sub>H<sub>42</sub>N<sub>2</sub>O<sub>9</sub>SNa), 641.2509; found, 641.2501.

(3*aS*,3*bR*,4*R*,7*aS*,8*aS*)-6,6-Dioxidoctahydro-2*H*-furo[2,3-*b*]thiopyrano[4,3-*d*]furan-4-yl ((2*S*,3*R*)-3-Hydroxy-4-(*N*-isobutyl-4-methoxyphenylsulfonamido)-1-phenylbutan-2-yl)carbamate (**16h**). The indicated inhibitor was obtained following the general procedure outlined above for inhibitor **16a**. The product was obtained as a mixture of diastereomers (**16h/16i**) (61% yield). **16h/16i** were separated by chiral HPLC, and titled inhibitor **16h** was determined to be >95%. Column ChiralPak IC, hexanes/IPA (52–48%, 20 min), 2.5 mL/min, 24 °C, retention time **16h** = 6.38 min.  $R_f = 0.28$  (50% ethyl acetate/hexanes); <sup>1</sup>H NMR (400 MHz, CDCl<sub>3</sub>)  $\delta$  7.75 (d,  $J = 5.4$  Hz, 2H), 7.27–7.25 (m, 5H), 6.99 (d,  $J = 6.0$  Hz, 2H), 5.69 (d,  $J = 5.5$  Hz, 1H), 5.58 (d,  $J = 5.5$  Hz, 1H), 5.43 (d,  $J = 9.1$  Hz, 1H), 5.37 (d,  $J = 9.3$  Hz, 1H), 5.19–5.10 (m, 2H), 4.08–3.98 (m, 1H), 3.95–3.88 (m, 1H), 3.86 (s, 3H), 3.83–3.71 (m, 3H), 3.68–3.49 (m, 1H), 3.40–3.30 (m, 1H), 3.28–3.18 (m, 2H), 3.20–3.05 (m, 2H), 3.05–2.91 (m, 1H), 2.91–2.69 (m, 1H), 2.50 (dd,  $J = 13.4$ , 9.7 Hz, 1H), 2.21–2.10 (m, 1H), 1.92–1.87 (m, 1H), 1.83–1.73 (m, 1H), 1.72–1.51 (m, 1H), 0.92 (d,  $J = 8.8$  Hz, 3H), 0.88 (d,  $J = 6.8$  Hz, 3H); <sup>13</sup>C NMR (100 MHz, CDCl<sub>3</sub>)  $\delta$  164.2, 156.4, 143.3, 129.7, 128.5, 128.4, 127.9, 114.4, 109.1, 74.9, 72.6, 71.8, 68.7, 57.7, 55.9, 50.2, 43.0, 41.4, 37.1, 32.0, 29.2, 29.0, 27.3, 27.1, 23.9, 20.1, 19.8; HRMS ( $m/z$ ) [ $M + Na$ ]<sup>+</sup> calcd for (C<sub>31</sub>H<sub>42</sub>N<sub>2</sub>O<sub>10</sub>S<sub>2</sub>Na), 689.2178; found, 689.2169.

(3*aS*,3*bS*,4*S*,7*aR*,8*aR*)-6,6-Dioxidoctahydro-2*H*-furo[2,3-*b*]thiopyrano[4,3-*d*]furan-4-yl ((2*S*,3*R*)-3-Hydroxy-4-(*N*-isobutyl-4-methoxyphenylsulfonamido)-1-phenylbutan-2-yl)carbamate (**16i**). Retention time = 8.02 min.  $R_f = 0.28$  (50% ethyl acetate/hexanes); <sup>1</sup>H NMR (400 MHz, CDCl<sub>3</sub>)  $\delta$  7.73 (d,  $J = 5.1$  Hz, 2H), 7.28–7.26 (m, 5H), 6.98 (d,  $J = 8.3$  Hz, 2H), 5.69 (d,  $J = 5.5$  Hz, 1H), 5.58 (d,  $J = 5.5$  Hz, 1H), 5.43 (d,  $J = 9.1$  Hz, 1H), 5.37 (d,  $J = 9.3$  Hz, 1H), 5.19–5.10 (m, 2H), 4.08–3.98 (m, 1H), 3.95–3.88 (m, 1H), 3.86 (s, 3H), 3.83–3.71 (m, 3H), 3.68–3.49 (m, 1H), 3.40–3.30 (m, 1H), 3.28–3.18 (m, 2H), 3.20–3.05 (m, 2H), 3.05–2.91 (m, 1H), 2.91–2.69 (m, 1H), 2.50 (dd,  $J = 13.4$ , 9.7 Hz, 1H), 2.21–2.10 (m, 1H), 1.89 (dq,  $J = 13.9$ , 7.2, 6.7 Hz, 1H), 1.83–1.73 (m, 1H), 1.72–1.51 (m, 1H), 0.92 (d,  $J = 4.5$  Hz, 3H), 0.87 (d,  $J = 2.8$  Hz, 3H); <sup>13</sup>C NMR (100 MHz, CDCl<sub>3</sub>)  $\delta$  164.3, 156.4, 143.3, 129.7, 128.4, 128.3, 127.9, 113.8, 109.1, 74.9, 72.6, 71.8, 68.5, 57.7, 55.9, 50.2, 43.0, 41.4, 37.2, 32.1, 31.8, 30.9, 29.2, 28.9, 27.3, 27.1, 23.8, 20.1, 19.8; HRMS ( $m/z$ ) [ $M + Na$ ]<sup>+</sup> calcd for (C<sub>31</sub>H<sub>42</sub>N<sub>2</sub>O<sub>10</sub>S<sub>2</sub>Na), 689.2178; found, 689.2170.

**Determination of the X-ray Structure of the Inhibitor 16a–HIV-1 Protease Complex.** The HIV-1 protease was expressed and purified as previously described.<sup>29,30</sup> The protease–inhibitor complex was crystallized at room temperature by the hanging-drop vapor-diffusion method with well solutions of 1.15 M ammonium chloride and 0.1 M sodium acetate buffer (pH 5.5). Diffraction data were collected on a single crystal cooled to 90 K at the SER-CAT BM beamline 22,



Advanced Photon Source, Argonne National Laboratory (Chicago, IL), with an X-ray wavelength of 1.0 Å, and the data were processed by HKL-2000<sup>31</sup> with Rmerge of 6.1%. The PR structure was used in molecular replacement by PHASER<sup>32,33</sup> in the CCP4i suite<sup>34,35</sup> and was refined to a 1.29 Å resolution using SHELX-97<sup>36,37</sup> and COOT<sup>38</sup> for manual modification. PRODRG-2<sup>39</sup> was used to construct the inhibitor and the restraints for refinement. Alternative conformations were modeled, anisotropic atomic displacement parameters (B factors) were applied for all atoms including solvent molecules, and hydrogen atoms were added in the final round of the refinement. The final refined solvent structure was composed of 1 sodium ion, 2 chloride ions, 3 acetate ions, 2 glycerol molecules, and 220 water molecules. The crystallographic statistics are listed in Table S1 in the Supporting Information. The coordinates and structure factors of the PR with 16a complex have been deposited in Protein Data Bank<sup>40</sup> under code 4KB9.

## ■ ASSOCIATED CONTENT

### ● Supporting Information

HPLC and HRMS data for inhibitors 16a–16i. Crystallographic data collection and refinement statistics for inhibitor 16a. This material is available free of charge via the Internet at <http://pubs.acs.org>.

### Accession Codes

The PDB accession code for 16a-bound HIV-1 protease X-ray structure is 4KB9.

## ■ AUTHOR INFORMATION

### Corresponding Author

\*E-mail: [akghosh@purdue.edu](mailto:akghosh@purdue.edu); Phone: (765)-494-5323; Fax: (765)-496-1612.

### Notes

The authors declare no competing financial interest.

## ■ ACKNOWLEDGMENTS

This research was supported by the National Institutes of Health (grant nos. GM53386 to A.K.G. and GM62920 to I.T.W.). This work was also supported by the Intramural Research Program of the Center for Cancer Research, National Cancer Institute, National Institutes of Health and was supported in part by a Grant-in-Aid for Scientific Research (Priority Areas) from the Ministry of Education, Culture, Sports, Science, and Technology of Japan (Monbu Kagakusho), a Grant for Promotion of AIDS Research from the Ministry of Health, Welfare, and Labor of Japan, and the Grant to the Cooperative Research Project on Clinical and Epidemiological Studies of Emerging and Reemerging Infectious Diseases (Renkei Jigyo) of Monbu-Kagakusho. We thank Dr. Kalapala Venkateswara Rao (Purdue University) for helpful discussions.

## ■ ABBREVIATIONS:

PI, protease inhibitor; APV, amprenavir; DRV, darunavir; SQV, saquinavir; bis-THF, bis-tetrahydrofuran; MDR, multidrug resistant

## ■ REFERENCES

- (1) Hue, S.; Gifford, R. J.; Dunn, D.; Fernhill, E.; Pillay, D. U.K. Demonstration of Sustained Drug-Resistant Human Immunodeficiency Virus Type 1 Lineages Circulating among Treatment-Naïve Individuals. *J. Virol.* **2009**, *83*, 2645–2654.
- (2) Conway, B. HAART in Treatment-Experienced Patients in the 21st Century: The Audacity of Hope. *Future Virol.* **2009**, *4*, 39–41.
- (3) Little, S. J.; Holte, S.; Routy, J. P.; Daar, E. S.; Markowitz, M.; Collier, A. C.; Koup, R. A.; Mellors, J. W.; Connick, E.; Conway, B.

Kilby, M.; Wang, L.; Whitcomb, J. M.; Hellmann, N. S.; Richman, D. Antiretroviral-Drug Resistance among Patients Recently Infected with HIV. *N. Engl. J. Med.* **2002**, *347*, 385–394.

(4) Ghosh, A. K.; Dawson, Z. L.; Mitsuya, H. Darunavir, a Conceptually New HIV-1 Protease Inhibitor for the Treatment of Drug-Resistant HIV. *Bioorg. Med. Chem.* **2007**, *15*, 7576–7580.

(5) Ghosh, A. K.; Chapsal, B. D.; Weber, I. T.; Mitsuya, H. Design of HIV Protease Inhibitors Targeting Protein Backbone: An Effective Strategy for Combating Drug Resistance. *Acc. Chem. Res.* **2008**, *41*, 78–86.

(6) Ghosh, A. K.; Sridhar, P. R.; Kumaragurubaran, N.; Koh, Y.; Weber, I. T.; Mitsuya, H. Bis-Tetrahydrofuran: A Privileged Ligand for Darunavir and a New Generation of HIV Protease Inhibitors That Combat Drug Resistance. *ChemMedChem.* **2006**, *1*, 939–950.

(7) Ghosh, A. K.; Xu, C.-X.; Rao, K. V.; Baldrige, A.; Agniswamy, J.; Wang, Y.-F.; Weber, I. T.; Aoki, M.; Miguel, S. G. P.; Amano, M.; Mitsuya, H. Probing Multidrug-Resistance and Protein–Ligand Interactions with Oxatricyclic Designed Ligands in HIV-1 Protease Inhibitors. *ChemMedChem* **2010**, *5*, 1850–1854.

(8) Zhang, H.; Wang, Y. F.; Shen, C.-H.; Agniswamy, J.; Rao, K. V.; Xu, X.; Ghosh, A. K.; Harrison, R. W.; Weber, I. T. Novel P2 Tris-Tetrahydrofuran Group in Antiviral Compound 1 (GRL-0519) Fills the S2 Binding Pocket of Selected Mutants of HIV-1 Protease. *J. Med. Chem.* **2013**, *56*, 1074–1083.

(9) Amano, M.; Tojo, Y.; Salcedo-Gómez, P. M.; Campbell, J. R.; Das, D.; Aoki, M.; Xu, C.-X.; Rao, K. V.; Ghosh, A. K.; Mitsuya, H. GRL-0519, a Novel Oxatricyclic Ligand-Containing Nonpeptidic HIV-1 Protease Inhibitor (PI), Potentially Suppresses Replication of a Wide Spectrum of Multi-PI-Resistant HIV-1 Variants In Vitro. *Antimicrob. Agents Chemother.* **2013**, *57*, 2036–2046.

(10) Ghosh, A. K.; Chapsal, B.; Mitsuya, H. Darunavir, a New PI with Dual Mechanism: From a Novel Drug Design Concept to New Hope Against Drug-Resistant HIV. In *Aspartic Acid Proteases as Therapeutic Targets*; Ghosh, A., Ed.; Wiley-VCH: Weinheim, Germany, 2010; pp 205–243.

(11) Corey, E. J.; Ghosh, A. K. Mn(III)-Promoted Annulation of Enol Ethers to Fused or Spiro 2-Cyclopentanones. *Tetrahedron Lett.* **1987**, *28*, 175–178.

(12) CCDC 940709 (12) and CCDC 940708 (13) contain the supplementary crystallographic data for this Article. These data can be obtained free of charge from The Cambridge Crystallographic Data Center via [www.ccdc.cam.ac.uk/data\\_request/cif](http://www.ccdc.cam.ac.uk/data_request/cif).

(13) Thompson, H. W.; Naipawer, R. E. Stereochemical Control of Reductions III. An Approach to Group Haptophilicities. *J. Am. Chem. Soc.* **1973**, *95*, 6379–6386.

(14) Bianchi, D.; Cesti, P.; Battistel, E. Anhydrides as Acylating Agents in Lipase-Catalyzed Stereoselective Esterification of Racemic Alcohols. *J. Org. Chem.* **1988**, *53*, 5531–5534.

(15) Ghosh, A. K.; Chen, Y. Synthesis and Optical Resolution of High Affinity P2-Ligands for HIV-1 Protease Inhibitors. *Tetrahedron Lett.* **1995**, *36*, 505–508.

(16) Dale, J. A.; Dull, D. L.; Mosher, H. S.  $\alpha$ -Methyl- $\alpha$ -Trifluoromethylphenylacetic Acid, a Versatile Reagent for the Determination of Enantiomeric Composition of Alcohols and Amines. *J. Org. Chem.* **1969**, *34*, 2543–2549.

(17) Bornscheuer, U. T.; Kazlauskas, R. J. *Hydrolases in Organic Synthesis*; Wiley-VCH: Weinheim, Germany, 1999.

(18) Passet, M.; Mailhol, D.; Coquerel, Y.; Rodriguez, J. Diazo-Transfer Reactions to 1,3-Dicarbonyl Compounds with Tosyl Azide. *Synthesis* **2011**, *16*, 2549–2552.

(19) Altenbach, R. J.; Brune, M. E.; Buckner, S. A.; Coghlan, M. J.; Daza, A. V.; Fabiyi, A.; Gopalakrishnan, M.; Henry, R. F.; Khilevich, A.; Kort, M. E.; Milicic, I. Effects of Substitution on 9-(3-Bromo-4-fluorophenyl)-5,9-dihydro-3H,4H-2,6-dioxo-4-azacyclopenta[b]-naphthalene-1,8-dione, a Dihydropyridine ATP-Sensitive Potassium Channel Opener. *J. Med. Chem.* **2006**, *49*, 6869–6887.

(20) Terasawa, T.; Okada, T. Novel Heterocyclic Synthons. Synthesis and Properties of Thia- and Oxacyclohexane-3,5-diones. *J. Org. Chem.* **1977**, *42*, 1163–1169.

- (21) Kitamura, M.; Tashiro, N.; Satoshi Miyagawa, S.; Tatsuo Okauchi, T. 2-Azido-1,3-dimethylimidazolium Salts: Efficient Diazo-Transfer Reagents for 1,3-Dicarbonyl Compounds. *Synthesis* **2011**, *7*, 1037–1044.
- (22) Webb, K. S. A Mild, Inexpensive and Practical Oxidation of Sulfides. *Tetrahedron Lett.* **1994**, *35*, 3457–3460.
- (23) Volkmann, R. A.; Kelbaugh, P. R.; Nason, D. M.; Jasys, V. 2-Thioalkyl Penems: An Efficient Synthesis of Sulopenem, a (5*R*,6*S*)-6-(1(*R*)-Hydroxyethyl)-2-[(*cis*-1-oxo-3-thiolanyl)thio]-2-penem Antibacterial. *J. Org. Chem.* **1992**, *57*, 4352–4361.
- (24) Pirrung, M. C.; Zhang, J.; Lackey, K.; Sternbach, D. D.; Brown, F. Reactions of a Cyclic Rhodium Carbenoid with Aromatic Compounds and Vinyl Ethers. *J. Org. Chem.* **1995**, *60*, 2112–2124.
- (25) Müller, P.; Allenbach, Y. F.; Bernardinelli, G. On the Enantioselectivity of Transition Metal-Catalyzed 1,3-Cycloadditions of 2-Diazocyclohexane-1,3-diones. *Helv. Chim. Acta* **2003**, *86*, 3164–3172.
- (26) Ghosh, A. K.; Chapsal, B. D.; Baldrige, A.; Steffey, M. P.; Walters, D. E.; Koh, Y.; Amano, M.; Mitsuya, H. Design and Synthesis of Potent HIV-1 Protease Inhibitors Incorporating Hexahydrofurofuranol-Derived High Affinity P2 Ligands: Structure–Activity Studies and Biological Evaluation. *J. Med. Chem.* **2011**, *54*, 622–634.
- (27) Toth, M. V.; Marshall, G. R. A Simple Continuous Fluorometric Assay for HIV Protease. *Int. J. Pept. Protein Res.* **1990**, *36*, 544–550.
- (28) Koh, Y.; Nakata, H.; Maeda, K.; Ogata, H.; Bilcer, G.; Devasamudram, T.; Kincaid, J. F.; Boross, P.; Wang, Y.-F.; Tie, Y.; Volarath, P.; Gaddis, L.; Harrison, R. W.; Weber, I. T.; Ghosh, A. K.; Mitsuya, H. A Novel Bis-Tetrahydrofuranylethane-Containing Non-Peptide Protease Inhibitor (PI) UIC-94017 (TMC114) Potent against Multi-PI-Resistant HIV In Vitro. *Antimicrob. Agents Chemother.* **2003**, *47*, 3123–3129.
- (29) Tie, Y.; Boross, P. I.; Wang, Y.-F.; Gaddis, L.; Hussain, A. K.; Leshchenko, S.; Ghosh, A. K.; Louis, J. M.; Harrison, R. W.; Weber, I. T. High Resolution Crystal Structures of HIV-1 Protease with a Potent Non-Peptide Inhibitor (UIC-94017) Active against Multi-Drug-Resistant Clinical Strains. *J. Mol. Biol.* **2004**, *338*, 341–352.
- (30) Mahalingam, B.; Louis, J. M.; Hung, J.; Harrison, R. W.; Weber, I. T. Structural Implications of Drug-Resistant Mutants of HIV-1 Protease: High Resolution Crystal Structures of the Mutant Protease/Substrate Analog Complexes. *Proteins* **2001**, *43*, 455–464.
- (31) Otwinowski, Z.; Minor, W. Processing of X-ray Diffraction Data Collected in Oscillation Mode. In *Methods in Enzymology: Macromolecular Crystallography, Part A*; Carter, C. W., Jr., Sweet, R. M., Eds.; Academic Press: New York, 1997; Vol. 276, pp 307–326.
- (32) Shen, C. H.; Wang, Y. F.; Kovalevsky, A. Y.; Harrison, R. W.; Weber, I. T. Amprenavir Complexes with HIV-1 Protease and Its Drug-Resistant Mutants Altering Hydrophobic Clusters. *FEBS J.* **2010**, *277*, 3699–3714.
- (33) McCoy, A. J.; Grosse-Kunstleve, R. W.; Adams, P. D.; Winn, M. D.; Storoni, L. C.; Read, R. J. Phaser Crystallographic Software. *J. Appl. Crystallogr.* **2007**, *40*, 658–674.
- (34) Collaborative Computational Project, Number 4. The CCP4 Suite: Programs for Protein Crystallography. *Acta Crystallogr., Sect. D* **1994**, *50*, 760–763.
- (35) Potterton, E.; Briggs, P.; Turkenburg, M.; Dodson, E. A Graphical User Interface to the CCP4 Program Suite. *Acta Crystallogr., Sect. D* **2003**, *59*, 1131–1137.
- (36) Sheldrick, G. M. A Short History of SHELX. *Acta Crystallogr., Sect. A* **2008**, *64*, 112–122.
- (37) Sheldrick, G. M.; Schneider, T. R. SHELXL: High Resolution Refinement. *Methods Enzymol.* **1997**, *277*, 319–343.
- (38) Emsley, P.; Cowtan, K. Coot: Model-Building Tools for Molecular Graphics. *Acta Crystallogr., Sect. D* **2004**, *60*, 2126–2132.
- (39) Schuettelkopf, A. W.; van Aalten, D. M. F. PRODRG: A Tool for High-Throughput Crystallography of Protein-Ligand Complexes. *Acta Crystallogr., Sect. D* **2004**, *60*, 1355–1363.
- (40) Berman, H. M.; Westbrook, J.; Feng, Z.; Gilliland, G.; Bhat, T. N.; Weissig, H.; Shindyalov, I. N.; Bourne, P. E. The Protein Data Bank. *Nucleic Acids Res.* **2000**, *28*, 235–242.



RESEARCH ARTICLE

## Preformulation studies of EFdA, a novel nucleoside reverse transcriptase inhibitor for HIV prevention

Wei Zhang<sup>1,2</sup>, Michael A. Parniak<sup>3</sup>, Hiroaki Mitsuya<sup>4,5</sup>, Stefan G. Sarafianos<sup>6</sup>, Phillip W. Graebing<sup>1</sup>, and Lisa C. Rohan<sup>1,2</sup>

<sup>1</sup>Magee Womens Research Institute, University of Pittsburgh, Pittsburgh, PA, USA, <sup>2</sup>Department of Pharmaceutical Sciences, School of Pharmacy, University of Pittsburgh, Pittsburgh, PA, USA, <sup>3</sup>Department of Microbiology and Molecular Genetics, School of Medicine, University of Pittsburgh, Pittsburgh, PA, USA, <sup>4</sup>Department of Hematology and Infectious Diseases, Kumamoto University, Kumamoto, Japan, <sup>5</sup>Experimental Retrovirology Section, HIV/AIDS Malignancy Branch, National Institutes of Health, Bethesda, MD, USA, and <sup>6</sup>Department of Molecular Microbiology & Immunology, and Biochemistry, University of Missouri, Columbia, MI, USA

### Abstract

4'-Ethylnyl-2-fluoro-2'-deoxyadenosine (EFdA) is a novel nucleoside analog of great interest because of its superior activity against wild-type and multidrug-resistant HIV-1 strains, and favorable safety profiles *in vitro* and *in vivo*. The aim of this work was to provide preformulation information of EFdA important for delivery system development. A simple, accurate and specific reverse-phase high performance liquid chromatographic (RP-HPLC) method with UV detection was developed for quantification of EFdA. In addition, physicochemical characterizations including pH solubility profile, octanol/water partition coefficient (Log  $P_{o/w}$ ), DSC analysis, field emission scanning electron microscopy, and stability studies under various conditions were conducted. EFdA existed in planar or flake shape, with a melting point of  $\sim 130^\circ\text{C}$ , and had a pH dependent solubility. The log  $P_{o/w}$  value of EFdA was  $-1.19$ . The compound was stable upon exposure to pH levels from 3 to 9 and showed good stability at elevated temperature ( $65^\circ\text{C}$ ). *In vitro* cytotoxicity assessments were performed in two different epithelial cell lines. In cell-based studies, the EFdA selectivity index (50% cytotoxic concentration [ $CC_{50}$ ] values/50% effective concentration [ $EC_{50}$ ]) was found to be greater than  $1 \times 10^3$ . Permeability studies using cell- and tissue-based models showed that EFdA had an apparent permeability coefficient ( $P_{app}$ )  $< 1 \times 10^{-6}$  cm/s and that the paracellular pathway was the dominant transport route for EFdA. Overall, EFdA possesses favorable characteristics for further formulation development.

### Keywords

Caco-2 cells, EFdA, permeability, preformulation, solubility, transport

### History

Received 1 February 2013  
Revised 17 May 2013  
Accepted 22 May 2013  
Published online 10 July 2013

### Introduction

As of 2010, there were an estimated 34 million people were living with HIV worldwide, with nearly 70% of these individuals in sub-Saharan Africa<sup>1</sup>. To date, HIV reverse transcriptase inhibitors, including non-nucleoside reverse transcriptase inhibitors (NNRTIs), nucleoside reverse transcriptase inhibitors (NRTIs) and nucleotide reverse transcriptase inhibitors (NtRTIs) are major components of highly active antiretroviral therapy (HAART) used as first-line therapies for the treatment of HIV infection. Although HAART has dramatically improved the quality of life and prognosis of patients infected by HIV-1, a number of side effects are associated with this therapy such as lipid and gastrointestinal abnormalities. Furthermore, this therapy can be associated with the development of HIV resistance. For these reasons new drugs are needed to maintain therapeutic options for patients failing on currently available therapies.

Furthermore, preventive measures such as microbicides (oral and topical pre-exposure prophylaxis) and vaccines are urgently needed to curb the continued spread of HIV infection. Advanced drug delivery systems and proper administration routes for anti-HIV compounds should be taken into consideration in order to prevent HIV transmission effectively, given that sexual transmission through the lower genital and rectal mucosa is a major pathway for HIV infection<sup>2</sup>. Currently, vaginal drug delivery has been widely used for different types of therapeutic agents such as antibacterials, antifungals, spermicides and steroids. At present, several promising vaginal microbicides are being explored for prevention of HIV-1 sexual transmission at the research and development or early clinical trial stage. These candidates consist of viral entry inhibitors (including broadly neutralizing monoclonal antibodies), reverse transcriptase inhibitors and integrase inhibitors. The most advanced of the microbicide candidates is the nucleotide reverse transcriptase inhibitor (NtRTI) tenofovir. A tenofovir gel product is currently being evaluated in a Phase III clinical trial (FACTS 001) as a topical microbicide to prevent HIV-1 infection. Previously it was evaluated in two Phase IIb trials (CAPRISA 004 and VOICE). The 1% tenofovir vaginal gel

Address for correspondence: Lisa C. Rohan, Magee Womens Research Institute, University of Pittsburgh, Pittsburgh, PA, USA. Tel: +1-412-641-6108. Fax: +1-412-641-6170. E-mail: rohanlc@upmc.edu

was found to reduce HIV-1 incidence by 39% in the CAPRISA 004 trial. However, the tenofovir vaginal gel arm in the VOICE clinical trial was discontinued for futility. In addition to gel products, intravaginal rings containing antiretrovirals such as zidovudine (nucleoside reverse transcriptase inhibitor, NRTI), dapivirine (non-nucleoside reverse transcriptase inhibitor, NNRTI), tenofovir and MIV-150 (NNRTI) and vaginal films containing tenofovir, dapivirine, RC-101 (retrocyclin analog) and IQP-0528 are under development by several research groups as they may potentially provide improved user compliance and adherence<sup>3–11</sup>. As an ideal anti-HIV microbicide, it should possess the properties<sup>11</sup>: (1) potent activity against most HIV strains and other sexually transmitted pathogens; (2) effective against both cell-free and cell-associated HIV; (3) no effect on the integrity of vagina and cervical mucosal epithelium; (4) no effect on vaginal commensal flora, especially lactobacilli; (5) resistant to acidic pH and stable at higher, tropical temperatures; (6) odorless, colorless and tasteless and (7) easy to use and low cost.

Recently, a novel NRTI, 4'-ethynyl-2-fluoro-2'-deoxyadenosine (EFdA), was reported to exert highly potent antiretroviral activity both *in vitro*<sup>12–14</sup> and *in vivo*<sup>15,16</sup>. EFdA retains potent activity against a variety of drug-resistant and multi-drug resistant strains of HIV, and has very favorable toxicity profiles *in vitro*<sup>12</sup> and *in vivo*<sup>16</sup>. Thus, EFdA may be a very promising drug candidate for use in both HIV therapeutic and preventive modalities. In order to direct the development of EFdA in a vaginal pharmaceutical dosage form, it is important to assess the fundamental properties of the drug substance that are important factors for the development of a stable, safe, effective and marketable formulated product such as tablet, gel, film or ring. The aim of the present studies was to provide preclinical preformulation data for EFdA to facilitate the development of EFdA related drug delivery systems. To this end, we carried out a series of preformulation work including analytical method development and validation, physicochemical properties such as pH-solubility profile, Log  $P_{o/w}$ , field emission scanning electron microscopy, DSC analysis, pH and thermal stability, *in vitro* cytotoxicity and bioactivity, and drug permeability across cell- and human tissue-based models.

## Materials and methods

### Materials

EFdA was a generous gift from Yamasa Corp. (Chiba, Japan). BD Falcon™ cell culture inserts, methanol (HPLC grade), 1-octanol, DMSO, HEPES and fetal bovine serum (FBS) potassium bipthalate, potassium phosphate monobasic, potassium chloride, sodium chloride, certified 0.2 M sodium hydroxide and hydrochloric acid solutions were obtained from Fisher Scientific (Pittsburgh, PA). HBSS was purchased from Lonza (Walkersville, MD). MTT was purchased from Sigma-Aldrich (St. Louis, MO). Methanesulfonic acid was obtained from Acros (Morris Plains, NJ). Phosphate buffered saline (PBS, pH 7.4), RPMI1640, Dulbecco's modified Eagle medium (DMEM) and penicillin-streptomycin were purchased from Mediatech Inc (Manassas, VA). All other chemicals were analytical grade. Ultrapure water was obtained in-house from a MilliQ water purification unit.

### HPLC analysis

An HPLC system (Waters Corporation, Milford, MA) equipped with an auto injector (model 717), a quaternary pump (model 600), and a Photodiode Array Detector (PDA, model 2996) was used for analytical method development. Empower Pro 2 software was used to control the HPLC system. Separation of the

compound of interest was achieved by using a Zorbax Eclipse XDB C18 column (3.5  $\mu$ m, 100  $\times$  4.6 mm). The mobile phase consisted of (A) 0.4% phosphoric acid in MilliQ water and (B) methanol using a gradient elution of 10–40% B at 0–5 min, 40–60% B at 5–10 min 60% B at 10–11 min, 60–10% B at 11–13 min, and 10% B at 13–20 min at a flow rate of 0.8 ml/min. Sample injection volume was 10  $\mu$ l and EFdA was determined by UV detection at 260 nm. All experiments were performed at room temperature and the total area of peak was used to quantify EFdA.

## Physicochemical characterization

### pH-solubility profile

Buffer systems in the range of 3–9 were used for pH-solubility profile studies. Standard buffer solutions were 0.2 M and included acid phthalate buffer (pH 3.0 or 4.0), neutralized phthalate buffer (pH 5.0), PBS (pH 5.0, 6.0 or 7.0), and alkaline borate buffer (pH 9.0) prepared according to USP. In order to investigate the effect of ionic strength on the solubility of EFdA, the ionic strength of different buffer solutions at pH 4, 7 and 9 was adjusted to 0.5 and 1.0 by adding sodium chloride. An excess amount of EFdA was added to microcentrifuge tubes containing 1.0 ml of the different buffer solutions. The samples were mixed using a Multi-Purpose Rotator with moderate rotation speed at ambient temperature for 120 h. The samples were then filtered through a 0.2  $\mu$ m membrane filter and the filtrate was analyzed by HPLC as described above. All measurements were conducted in triplicate.

### Octanol/water partition coefficient (Log $P_{o/w}$ ) determination

Octanol-aqueous solutions comprising octanol and MilliQ water, acetate buffer (pH 4.1) or PBS (pH 7.4) in the ratio of 1:2 (v/v) were mixed and allowed to pre-saturate for 24 h at room temperature. Known amounts of EFdA were added to the different pre-saturated mixtures, and the samples were rotated end-over-end at room temperature for 120 h. Aliquots of the aqueous phase were withdrawn and assessed for EFdA content by HPLC. The concentration of EFdA in the octanol phase was calculated based on distribution of the known amount of EFdA into the aqueous phase. Log  $P_{o/w}$  was calculated as the logarithm of the ratio of EFdA concentration in the octanol to that in the aqueous phase. All determinations were done in duplicate. Calculated Log  $P_{o/w}$  (cLog  $P_{o/w}$ ) was determined using Marvin sketch software (version 5.5).

### Field emission scanning electron microscopy

Surface morphology of EFdA was imaged by field emission scanning electron microscopy system (Philips XL30 FEG) at an accelerating voltage of 10 kV. Samples for field emission scanning electron microscopy (FESEM) were mounted on aluminum holders by carbon conductive glue and coated with a platinum layer by platinum sputter coater before scanning.

### Differential scanning calorimetry

Differential Scanning Calorimetry (DSC) was performed using Perkin-Elmer DSC 7, TAC 7/DX Thermal Analysis Controller (Boston, MA), and Pyris software. DSC thermograms were obtained by heating from 30 to 300 °C at a heating rate of 20 °C/min under a constant nitrogen purge of 20 ml/min.

### X-ray diffraction

X-ray diffraction (XRD) analysis of EFdA powders was conducted by an X-ray diffractometer (Philips PW1830/00, the Netherlands) equipped with a Cu K $\alpha$  radiation source (40 kV, 30 mA,  $\lambda$  = 0.15406 nm). EFdA powders were pressed onto the

sample holder to form a thin EFdA layer. The samples were measured from 2.5° to 45° at a rate of 0.04°/s.

#### Polarized light microscopy

Microscopic observations were performed using the Zeiss Axioskop 40 inverted phase-contrast microscope with polarized light filter. Images were acquired using AxioCam MRc5 color video camera and analyzed using AxioVision Rel 4.7 software. EFdA powders were mounted on glass slides, smeared with cytooseal™ 60, covered with cover slips and observed under polarized light.

#### Dynamic vapor sorption

Dynamic vapor sorption (DVS) analysis was conducted at Micromeritics Pharmaceutical Services (Norcross, GA) using DVS-Intrinsic (Surface measurement systems Ltd, UK) to investigate hygroscopicity behavior of EFdA. A drying step at 0% relative humidity (RH) was started and held for at least 2 h at 40 °C. For typical hygroscopicity assessment, approximately 7 mg of sample was used and the experiment was performed under isothermal conditions at 25 °C. The relative humidity (%RH) is stepped from a low initial level (0 %RH) to a high level (90 %RH), then back down to 0 %RH. Data was collected using DVS-Intrinsic control software and exported to an Excel spreadsheet for graphing.

#### Stability study

Known concentrations of EFdA were prepared in various buffer solutions ranging from pH 3–9 and incubated at 25 °C in the dark to avoid complications from potential photo-decomposition. Aliquots were removed at various times over a period of 21 days and the amount of EFdA was quantified by HPLC. Thermal stability of EFdA was assessed by incubation of aqueous solutions of the drug at 25, 40 or 65 °C for up to 21 days. Oxidative stability was evaluated by incubating a solution of EFdA in 0.02% hydrogen peroxide. Photolytic stability was assessed by exposing an aqueous solution of EFdA to light (Philips Daylight, 20 W). In all stability studies, the EFdA levels were quantified at different incubation times and compared to those of the starting solution. All determinations were in triplicate.

#### In vitro cytotoxicity

Two human epithelial carcinoma cell lines, CaSki (cervical origin) and A 431 (epidermal origin), were obtained from ATCC and the cells were cultured at 37 °C with 5% CO<sub>2</sub> under fully humidified conditions. The A 431 cells were cultured in DMEM medium, supplemented with 10% fetal bovine serum (FBS), 100 IU/ml penicillin and 100 µg/ml streptomycin sulfate, and the CaSki cells were cultured in RPMI 1640 medium, supplemented with 10% FBS, 100 IU/ml penicillin and 100 µg/ml streptomycin sulfate.

CaSki and A 431 cells were seeded in 96-well plates at a density of  $1 \times 10^4$  cells per well, respectively. After 24 h of incubation at 37 °C, the growth medium was replaced with 200 µl medium containing the drug samples with concentrations ranging from 1 ng/ml to 50 µg/ml. After 24, 48 or 72 h incubation, cell survival was measured using MTT assay. Briefly, drug-containing medium was removed and 180 µl of fresh growth medium and 20 µl of MTT (5 mg/ml) solution were added to each well. The plate was incubated for an additional 4 h at 37 °C and the media was removed, and then 200 µl of DMSO was added to each well to dissolve any purple formazan crystals formed. The plates were vigorously shaken before measuring the relative color intensity. The absorbance at 595 nm of each well was measured by a microplate reader (Beckman Coulter® DTX 880, US).

#### Transport of EFdA across Caco-2 cell monolayers

Caco-2 cells were cultured in DMEM medium, supplemented with 10% FBS, 1% non-essential amino acid solution, 1% L-glutamine, 1% penicillin–streptomycin at 37 °C with 5% CO<sub>2</sub> under fully humidified conditions. The cells were grown to 90% confluence and harvested by trypsinization using a 0.25% trypsin and 0.02% EDTA solution. For transport studies, Caco-2 cells were seeded at a density of  $2.5 \times 10^5$  onto polycarbonate inserts (4.2 cm<sup>2</sup>) in 6-well tissue culture plates. The medium was changed every second day for the first week and then replaced daily. Caco-2 cell monolayers were used between days 21 and 24 post-seeding. Cell passages between 27 and 32 were used in the experiment. The quality of the monolayers grown on the permeable membrane was assessed before and after the transport studies by the transepithelial electrical resistance (TEER) of the monolayers at 37 °C using a Millicell-ERS apparatus (Millipore, Bedford, MA). Only monolayers displaying TEER values > 600 Ωcm<sup>2</sup> were used in transport studies<sup>17,18</sup>.

Bidirectional transport of EFdA, apical-to-basolateral (a-b, absorptive) and basolateral-to-apical (b-a, secretory) was measured using Caco-2 cell monolayers prepared as described above. The incubation medium was Hank's balanced salt solution (HBSS) buffered either with 10 mM methanesulfonic acid (pH 5.5 and 6.5), or with 25 mM HEPES (pH 7.4)<sup>19</sup>. Before each experiment, the cell monolayers were washed twice with HBSS and then the monolayers were preincubated at 37 °C for 20 min with HBSS at the appropriate pH, followed by the measurement of TEER values. To investigate the effect of apical pH on the transport of EFdA from a-b, 1.5 ml of HBSS (pH 5.5, 6.5 or 7.4) containing EFdA (25 µg/ml) was added onto the apical side and 2.0 ml of HBSS (pH 7.4) without the test compound was added on the basolateral side. Additionally, in order to investigate the bidirectional transport of EFdA across Caco-2 cell monolayers, an expanded concentration range of EFdA (2.5 ~ 250 µg/ml) was applied. Briefly, 1.5 ml of HBSS (pH 7.4) containing EFdA was added onto the apical side and 2.0 ml of HBSS (pH 7.4) without EFdA was added on the basolateral side. Conversely, for the determination of b-a transport, 2.0 ml of HBSS (pH 7.4) containing EFdA was added onto the basolateral side and 1.5 ml of HBSS (pH 7.4) without the drug was added on the apical side. The Caco-2 cell monolayers were incubated at 37 °C for 2 h with moderate shaking. 200 µl medium was taken from each donor or receptor compartment at 0, 15, 30, 45, 60, 90 and 120 min, and then the same volume of fresh HBSS (pH 7.4) was supplemented. After the final time point, TEER values were measured again. EFdA in all samples was analyzed using HPLC as described above.

The apparent permeability coefficient ( $P_{app}$ ; cm/s) of EFdA was determined from the amount of compound transported over time.  $P_{app}$  was calculated according to the following equation:

$$P_{app} = (dQ/dt)/(A \times C_0) \quad (1)$$

where  $dQ/dt$  is the steady-state flux (µg/s),  $A$  is the surface area of exposure (cm<sup>2</sup>) and  $C_0$  is the initial concentration in the donor chamber (µg/ml). The ratio of the transport in the b-a direction to that in the a-b direction was calculated in order to highlight any asymmetry in the transport of the compounds. Efflux ratio was calculated using the following equation:

$$\text{Efflux ratio} = P_{app(b-a)}/P_{app(a-b)} \quad (2)$$

#### Human tissue permeability study

Freshly excised human ectocervical tissue was obtained from the Tissue Procurement Facility at Magee-Womens Hospital under IRB approved protocol. Tissue samples were from 3 women with

median age of 40 years undergoing hysterectomy for benign conditions. For each tissue, three replicates were performed for permeability studies. All tissue specimens were obtained within 2 h of surgical excision. Tissues were held at 4 °C in Dulbecco's modified Eagle medium (DMEM) during transfer from surgery to the laboratory. Excessive stromal tissue was removed and the epithelial layer was isolated using a Thomas-Stadie Riggs tissue slicer (Thomas Scientific, Swedesboro, NJ). The thickness of each tissue was measured by placing the tissue between two slides and the thickness was measured using a micrometer.

Tissue permeability studies were conducted using a Franz cell system (PermeGear, Nazareth, PA). The Franz cell system was a two-compartment system consisting of an upper chamber (donor compartment) and a lower chamber (receptor compartment). The system was water-jacketed and temperature was maintained at 37 °C throughout the experiment via a circulating water bath. The isolated epithelial sections of each tissue were placed between the donor and receptor compartments with the epithelial side of the tissue oriented towards the donor compartment which provided a diffusion area of 0.385 cm<sup>2</sup>. PBS (pH 7.4) solution was used in the receptor chamber. The latter chamber (5.0 ml volume) was continuously stirred by a magnetic stir bar. The tissue was equilibrated with PBS in the donor compartment for 5 min prior to the permeability study. After the equilibration period, PBS was removed from the donor chamber and replaced with 450 µL of EFdA (500 µg/ml in PBS, pH 7.4). 50 µL was removed from the donor compartment for mass balance. At various time intervals over a 6 h period, 200 µL aliquots were removed from the receptor compartment. Receptor compartment medium was replenished with fresh medium after removal of each aliquot. EFdA in the receptor compartment aliquots was quantified by HPLC.

### Bioactivity analysis

Two types of bioactivity tests were carried out, (i) standard antiviral assessments in which cells were simultaneously exposed to varying concentrations of drug and HIV, with drug being present throughout the infection process and (ii) protective or memory effect assessments in which cells were pretreated with varying concentrations of drug for 16 h, then exogenous drug was removed by extensive washing and the cells exposed to HIV in the absence of exogenous drug. HIV replication was evaluated in single replication cycle HIV assays, using P4R5 HIV infection indicator cells (from Dr John Mellors, University of Pittsburgh). Cells were maintained in DMEM/10% FBS supplemented with puromycin (0.5 g/ml). P4R5 cells express CD4, CXCR4 and CCR5 as well as a  $\beta$ -galactosidase reporter gene under the control of an HIV LTR promoter. Viral infectivity was assessed in 96-well microplate assays seeded with P4R5 cells at a density of  $5 \times 10^3$  cells/well. Cells were inoculated with 25 ng HIV-1 p24/well and the extent of infection was evaluated 48 h post-infection using a fluorescence-based  $\beta$ -galactosidase detection assay. Briefly, infected cells were washed, then incubated with 100 µL lysis buffer (60 mM Na<sub>2</sub>HPO<sub>4</sub>, 40 mM NaH<sub>2</sub>PO<sub>4</sub> (pH 7.2), 1 mM MgSO<sub>4</sub>, 100 mM  $\beta$ -mercaptoethanol, 2% [v/v] Triton X-100) for 1 h at 37 °C.  $\beta$ -Galactosidase activity was assessed by addition of 50 µL 4-MUG to a final concentration of 0.5 mM, incubation for 1 h at 37 °C, and then quenched with 150 µL 0.2 M Na<sub>2</sub>CO<sub>3</sub> (pH 11.2). Fluorescence intensity was assessed with a SPECTRA max GEMINI XS dual-scanning microplate spectrofluorometer (Molecular Devices, Sunnyvale, CA) using an excitation wavelength of 355 nm and an emission wavelength of 480 nm, with cutoff filter set to 475 nm.

### Statistical analysis

Statistical analysis was performed by Student's *t*-test for two groups and one-way ANOVA for multiple groups. All results were

expressed as the mean  $\pm$  standard deviation (SD). A *p* value < 0.05 is considered statistically significant.

## Results and discussion

### Analytical method for EFdA

Figure 1(A) shows a typical chromatogram of EFdA, with a retention time of approximately 13 min. The purity angle of EFdA was less than the purity threshold, indicating that there is no evidence of spectral heterogeneity (Figure 1B). Linearity of the standard curve for quantification of EFdA was determined by linear least squares regression analysis of a plot of peak area versus EFdA concentration, using seven standard solutions of EFdA over a range of 0.2 ~ 200 µg/ml. Standard variation was < 1.5%. The Limit of Detection (LOD) and Limit of Quantification (LOQ) for EFdA were estimated at a signal-to-noise ratio (S/N) of 3:1 and 10:1, respectively. The LOD was 0.05 µg/ml and LOQ was determined to be 0.15 µg/ml. As presented in Figure 1(C), the maximum absorbance for EFdA was at 260 nm.

### Physicochemical characterization

The solubility of EFdA was found to be pH dependent (Figure 2A). An increase in pH from 3 to 6 resulted in a significant decrease in EFdA solubility (from  $1508.7 \pm 68.4$  to  $799.2 \pm 8.7$  µg/ml,  $p < 0.05$ ), indicating that EFdA may be partially protonated under acidic conditions. From pH 6–9, no obvious change in solubility was observed for EFdA. Figure 2(B) shows the solubility of EFdA as a function of ionic strength under three different pH conditions. At pH 4.0, increase in ionic strength from 0.2 to 1.0, resulted in a slight decrease in solubility of EFdA (from  $1620.8 \pm 55.9$  to  $1358.3 \pm 48.3$  µg/ml,  $p > 0.05$ ). As for pH 7.0 and 9.0, a statistically significant decrease in the solubility of EFdA was observed with increase in ionic strength ( $p < 0.05$ ), suggesting that the high concentration of the salts in the solution may have negative impact on the solubility of EFdA. Additionally, it was found that the solubility of EFdA in Vaginal Fluid Simulant (VFS, pH = 4.2) was 887.4 µg/ml, less than that of acid phthalate buffer (pH 4.0), possibly due to the increased ionic strength in VFS. EFdA was also found to be soluble in DMSO (> 20 mg/ml), ethanol (> 10 mg/ml) and acetonitrile (> 1 mg/ml), respectively.

Drug octanol/water partition coefficient ( $\log P_{o/w}$ ) is commonly used to estimate the potential for drug absorption.  $\log P_{o/w}$  describes the ability of a drug molecule to partition into a lipophilic phase, octanol, which is assumed to have comparable lipophilicity to that of biological membranes<sup>20</sup>. The experimental partition coefficients determined for water, PBS (pH 7.4) and acetate buffer (pH 4.1) were  $-1.19$ ,  $-0.85$  and  $-0.87$ , respectively, suggesting that EFdA was hydrophilic. In addition, the  $c\log P$  predicted by Marvin sketch software was  $-0.82$ , which correlates well with the experimental  $\log P_{o/w}$  ( $-1.19$ ).

FESEM was used to better understand the crystal structure for EFdA. The FESEM images (Figure 3A) showed that EFdA crystals existed in planar or flaky shape of a non-uniform particle size. Aggregates of crystals were also observed. As presented in Figure 3(B), two endothermic events were obtained in the EFdA DSC thermogram, one at 129.3 °C and the other at 228.7 °C. The first endothermic peak observed in DSC may be attributed to the melting of crystalline drug powder, while the second endothermic event at 228.7 °C followed by a small exothermic peak in DSC might be due to the thermal decomposition of EFdA at higher temperature. XRD analysis was also performed to elucidate the crystalline state of EFdA. It was observed that EFdA powder presented high crystallinity by its sharp and intense diffractive peaks at 4.8°, 9.5°, 14.4°, 19.3° and 24.2° (Figure 3C).

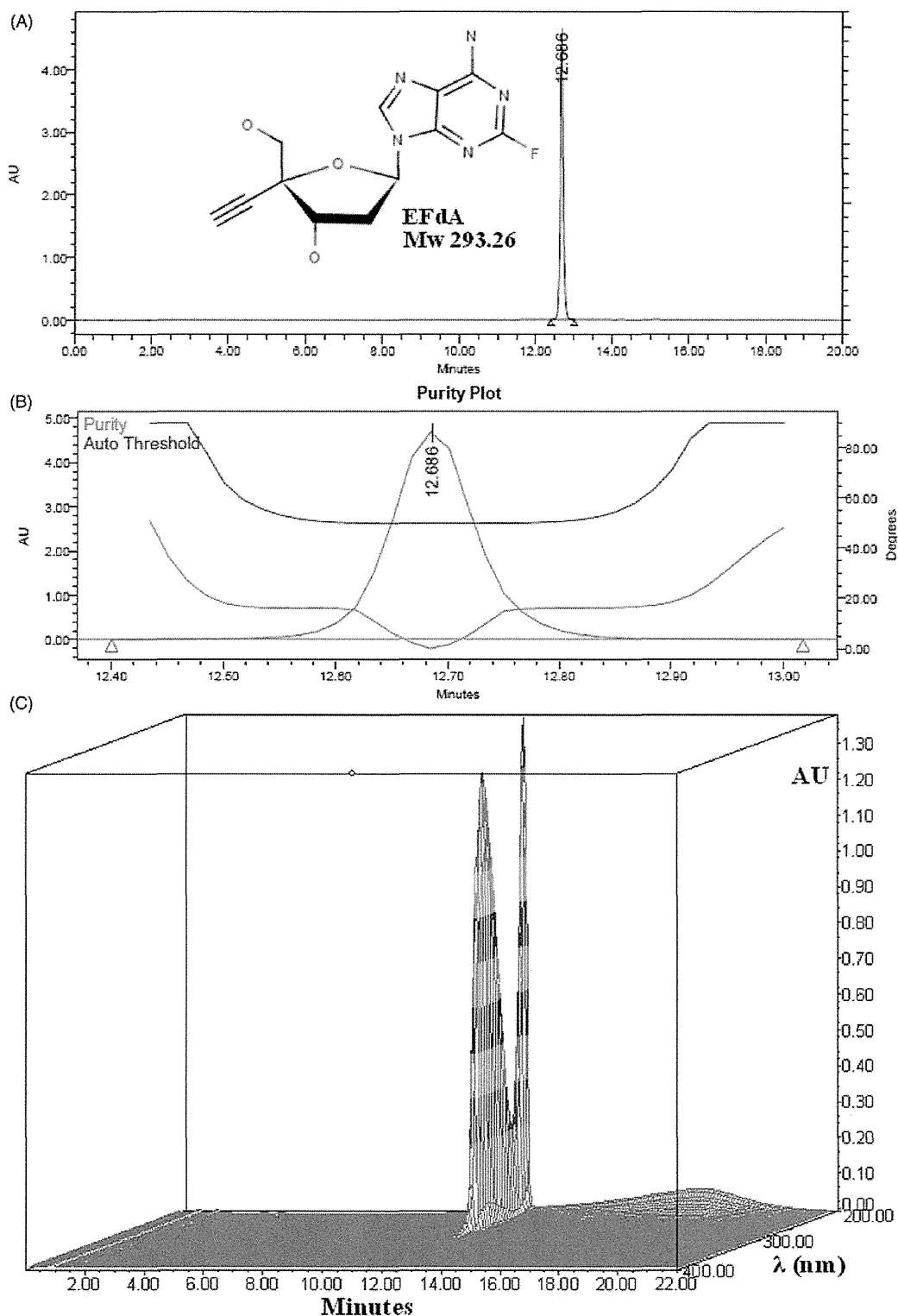


Figure 1. (A) Typical HPLC chromatogram of EFdA; (B) EFdA peak purity plot; (C) HPLC-DAD analysis of EFdA.

Crystallinity of EFdA was further confirmed by the presence of birefringence as observed using polarized light microscopy (Figure 3D). Results of dynamic vapor sorption study (Figure 4) indicated that EFdA was hygroscopic in nature and absorbed approximately 10% w/w moisture at 25°C/80% RH. Additionally, no sharp weight decrease was found in the desorption profile, suggesting that no hydrate was formed.

To elucidate the primary potential degradation pathways of EFdA, forced degradation studies (acid hydrolysis, base hydrolysis, photolysis, oxidative and thermal stability) were performed (Figure 5A–C). EFdA was very stable under all test conditions studied, with >95% of the drug remaining following exposure to accelerated condition. These data showed that EFdA was stable to light, 0.02% hydrogen peroxide and from pH 3.0–9.0. This data

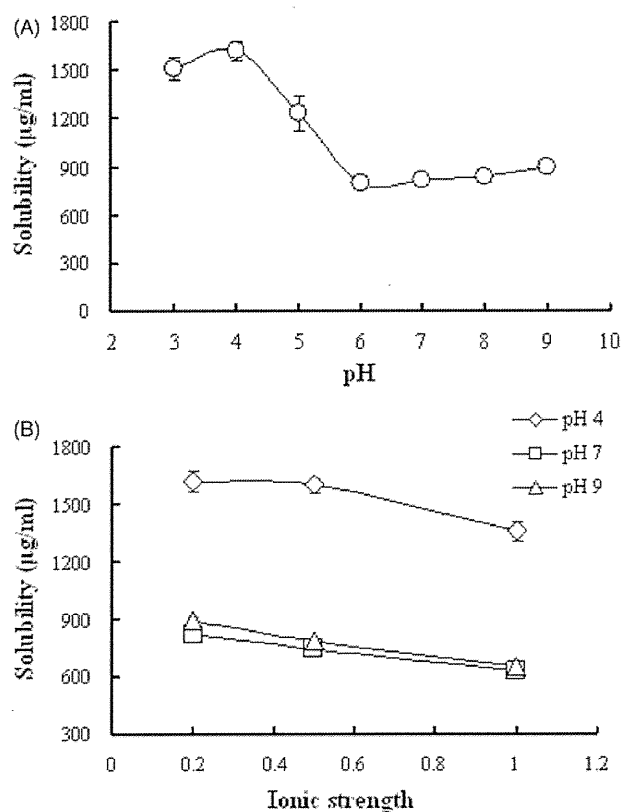


Figure 2. (A) pH-solubility profile of EFdA in different buffer solutions at various pH; (B) The effect of ionic strength on solubility of EFdA. Each point represents mean  $\pm$  SD ( $n=3$ ).

indicates that EFdA is stable at the physiological pH of the vagina (approximately 4.2). Additionally, its observed stability at relatively high temperature ( $\sim 65^\circ\text{C}$ ) is important for formulation development options such as solid dispersion preparation, film casting or nanoparticle fabrication.

#### In vitro cytotoxicity

In order to reduce the failure rate of a microbicide formulation in animal and clinical testing, it was important to assess potential safety issues, since local inflammation and disruption of epithelial barriers could lead to an increased risk of HIV acquisition or infection<sup>21</sup>. Therefore, cell viability assays were performed to determine the effect of EFdA exposure on CaSki and A 431 cell lines<sup>21–23</sup>. As illustrated in Figure 6(A), the EFdA provided a time-dependent slight increase in cytotoxicity in CaSki cells, with CC50 values greater than 50 µg/ml following 24 h treatment,  $47.81 \pm 12.40$  µg/ml at 48 h and  $41.11 \pm 8.78$  µg/ml at 72 h. Similar results were noted for the A 431 cell line (Figure 6B). The low cytotoxicity found in the present study correlates well with previous assessments of EFdA toxicity *in vitro*<sup>12–14</sup> and *in vivo*<sup>15,16</sup>.

#### Transport study across Caco-2 cell monolayers

Caco-2 cell monolayers have become the standard for *in vitro* prediction of intestinal drug permeability<sup>24,25</sup>. We used this system to evaluate EFdA transport. In our study, the pH of the apical medium was varied (5.5, 6.5 or 7.4) while maintaining the basolateral pH at 7.4 since it is known that oral absorption of drugs can be pH-dependent due to altered solubilities of weakly acidic or basic drugs<sup>26,27</sup>. As shown in Figure 7(A), the  $P_{app}$

values from apical side to basolateral side under different pH conditions were similar ( $3.67 \pm 0.27$ )  $\times 10^{-7}$  cm/s for pH 5.5, ( $4.36 \pm 0.09$ )  $\times 10^{-7}$  cm/s for pH 6.5 and ( $4.20 \pm 0.66$ )  $\times 10^{-7}$  cm/s for pH 7.4, indicating that the transport of EFdA across Caco-2 cell monolayers was independent of pH within the range studied. This is consistent with the constant solubility of EFdA over this pH range, as described above.

The influence of EFdA concentration on bidirectional transport of EFdA across Caco-2 cell monolayers was also determined. As presented in Figure 7(B), from apical to basolateral, the  $P_{app}$  (a-b) values of EFdA were ( $4.80 \pm 1.24$ )  $\times 10^{-7}$  and ( $5.95 \pm 1.44$ )  $\times 10^{-7}$  cm/s for 25 µg/ml and 250 µg/ml treatments, respectively. The differences between these values was not significant ( $p > 0.05$ ), suggesting that passive diffusion played a primary role in EFdA transport. As for the absorptive transport (a-b) of EFdA at the concentration of 2.5 µg/ml, no EFdA was detected in the receptor compartment, probably due to the LOD of HPLC method (0.05 µg/ml). For the transport of EFdA from basolateral to apical side, no significant difference in  $P_{app}$  (b-a) value was observed between low and medium concentration groups ( $p > 0.05$ ). However, the  $P_{app}$  (b-a) value obtained for the high concentration group was about 2-fold lower than those of low and medium concentration treatments, suggesting the possibility of a saturable transport process. These data suggest that there was no indication of saturation up to 25 µg/ml which was several orders of magnitude higher than the  $EC_{50}$  of EFdA ( $\sim 0.07$  nM)<sup>13</sup>. The efflux ratios for the medium and high concentration groups were 8.01 and 2.74, respectively, both greater than 1, suggesting that the efflux transporters such as P-glycoprotein (P-gp), multidrug resistance-associated proteins (MRPs) and breast cancer resistance protein (BRCP) or certain influx transporters expressed on the basolateral side might be involved in the transport of EFdA across Caco-2 cell monolayers.

#### Human tissue permeability study

The potent anti-HIV activity of EFdA suggests that it may have significant potential as a microbicide candidate for use in HIV prevention. For this application, EFdA could be formulated into dosage forms such as films, gels or rings for vaginal use by women. To understand the potential for systemic uptake of EFdA when delivered topically, a permeability study for EFdA using excised human ectocervical tissues was performed. EFdA transport through human ectocervical tissues was determined by quantitating the amount of EFdA found in the receptor compartment at predetermined time intervals using developed HPLC methods. The amount of drug which permeated the tissue was used to calculate the apparent permeability coefficient ( $P_{app}$ ) as described previously<sup>28</sup>. The average  $P_{app}$  value obtained from 3 separate excised human cervical tissues was ( $8.34 \pm 4.50$ )  $\times 10^{-7}$  cm/s (Figure 8A), which correlated well with previous results of transport studies conducted in Caco-2 cell monolayers. Additionally, both inter- and intra-patient variability were observed among EFdA diffusion profiles obtained from different human ectocervical explants. It is well known that lipophilic compounds are usually transported through the transcellular route while hydrophilic drugs are primarily transported through the paracellular pathway which consists of small watery channels and pores within the discontinuous or interrupted lipid membrane<sup>28</sup>. The average molecular size cutoff for the paracellular route of passive diffusion is approximately 500 Da<sup>29</sup>. Based on the negative Log  $P_{o/w}$  value of EFdA and permeability study results (Caco-2 cell monolayers and excised human cervical tissues), we propose that the paracellular route is the dominant pathway for EFdA to penetrate the vaginal epithelia. Furthermore, the lack of any significant morphological changes in human ectocervical



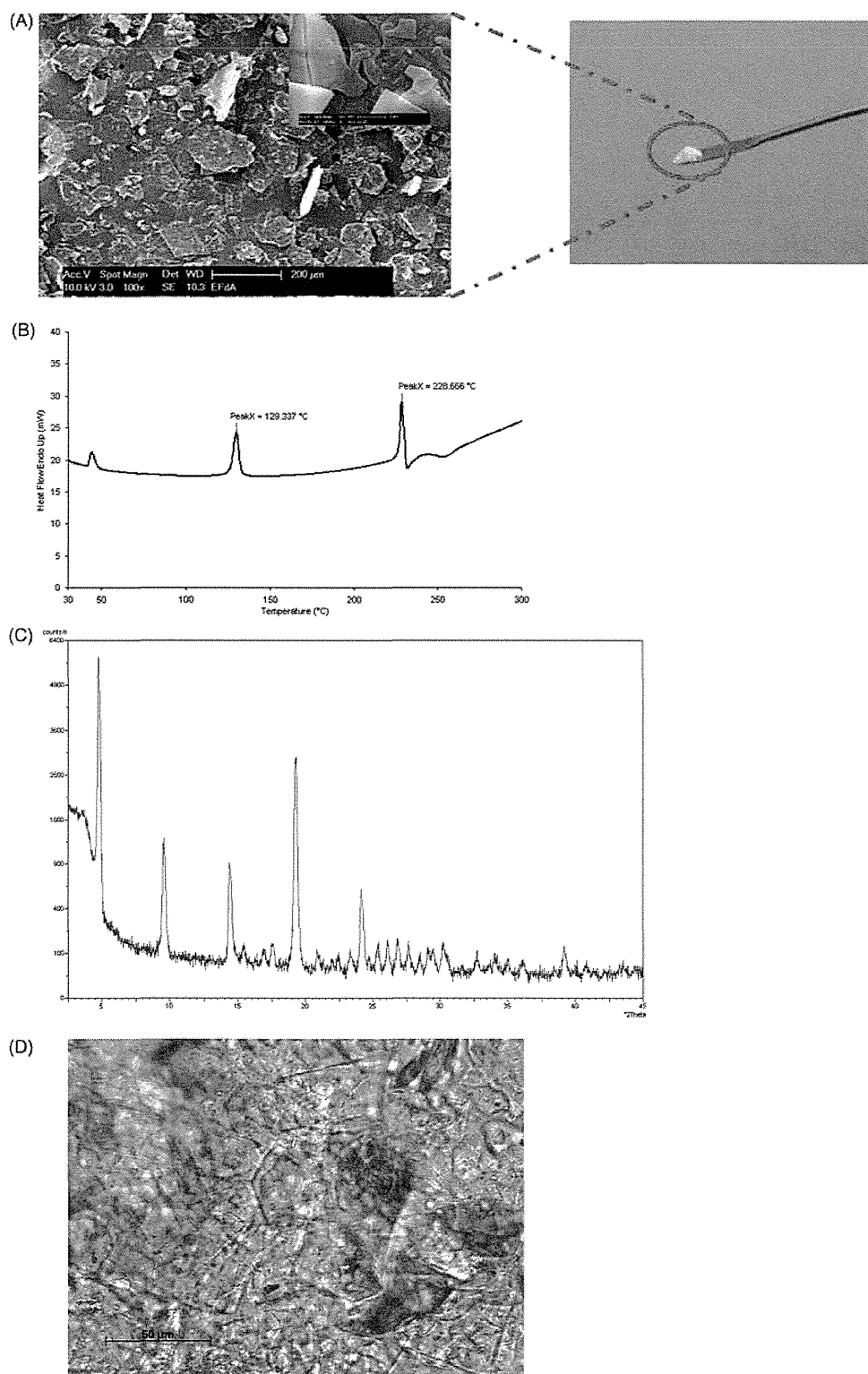


Figure 3. (A) Observation of drug powder by field emission scanning electron microscopy (FESEM). Insert shows FESEM image of EFdA with the scale bar = 2 μm. (B) DSC thermogram for EFdA. DSC analysis was performed with Perkin-Elmer DSC 7, TAC 7/DX Thermal Analysis Controller (Boston, MA), and Pyris software. (C) X-ray diffractograms of EFdA powders. X-ray diffraction was conducted by an X-ray diffractometer (Philips PW1830/00, Netherlands) equipped with a Cu K $\alpha$  radiation source (40 kV, 30 mA,  $\lambda = 0.15406$  nm). (D) Polarized light microscopic image of EFdA with the scale bar = 50 μm.

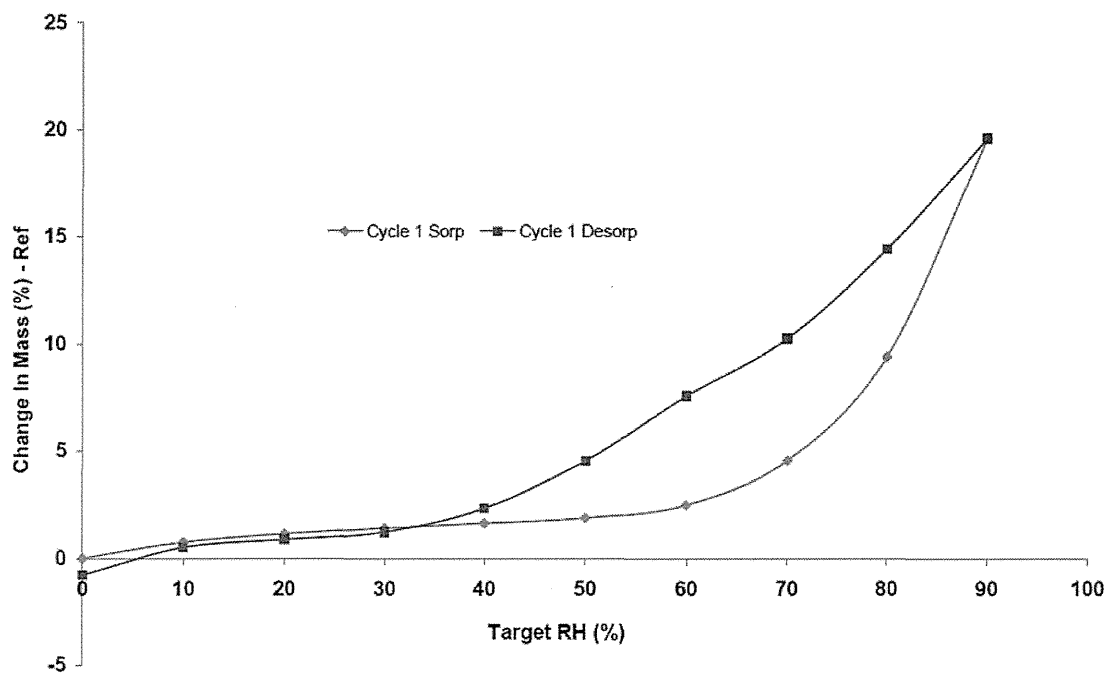
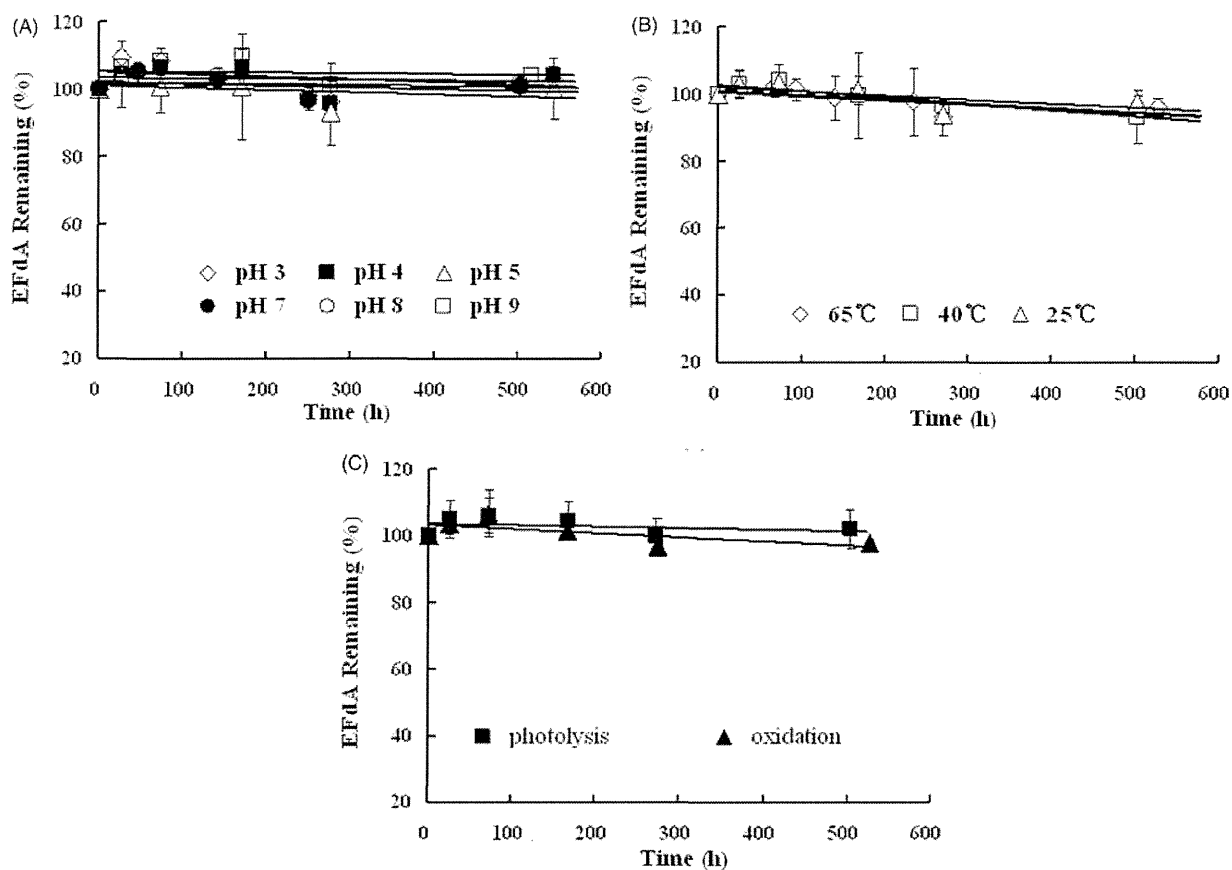


Figure 4. DVS isotherm plot of EFdA.

Figure 5. Kinetic stability of EFdA (200 µg/ml) in buffer solutions against time under different pH (A), temperature (B), light and oxidation (C) conditions. Each point represents mean  $\pm$  SD ( $n=3$ ).

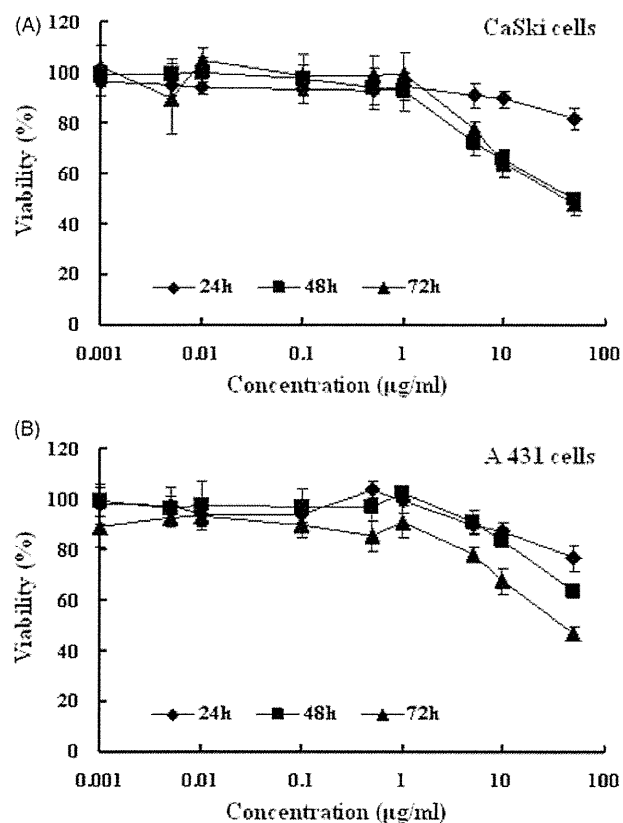


Figure 6. *In vitro* cytotoxicity of EFdA at various concentrations against CaSki (A) and A 431 (B) cell lines at 24, 48 and 72 h. Each point represents mean  $\pm$  SD ( $n = 8$ ).

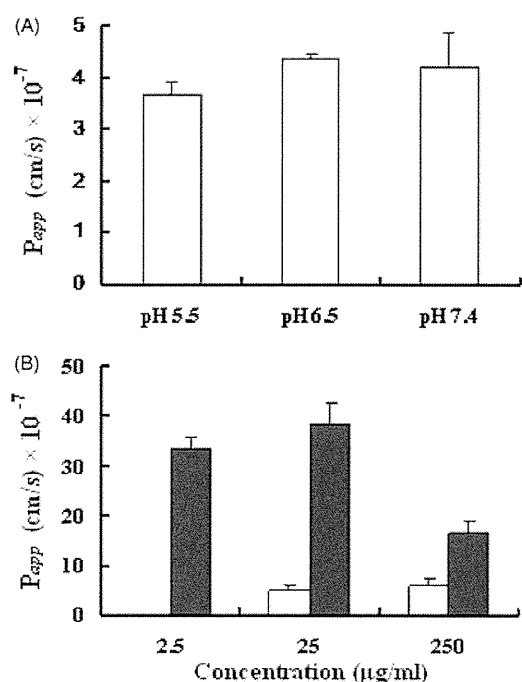


Figure 7. (A) Effect of pH on the apparent permeability coefficient ( $P_{app}$ ) of EFdA across Caco-2 monolayers. Caco-2 monolayers were incubated with 25  $\mu\text{g/ml}$  EFdA on the apical side at 37  $^{\circ}\text{C}$ . The pH of apical side was 5.5, 6.5, 7.4, and the pH of the basolateral side was maintained at pH 7.4. (B) Bidirectional transport of EFdA across Caco-2 cell monolayers at concentrations of 2.5, 25 or 250  $\mu\text{g/ml}$  (Open: a-b; Filled: b-a). The buffer pH was the same on both sides of the monolayer (pH 7.4). Each value indicates mean  $\pm$  SD ( $n = 3$ ).

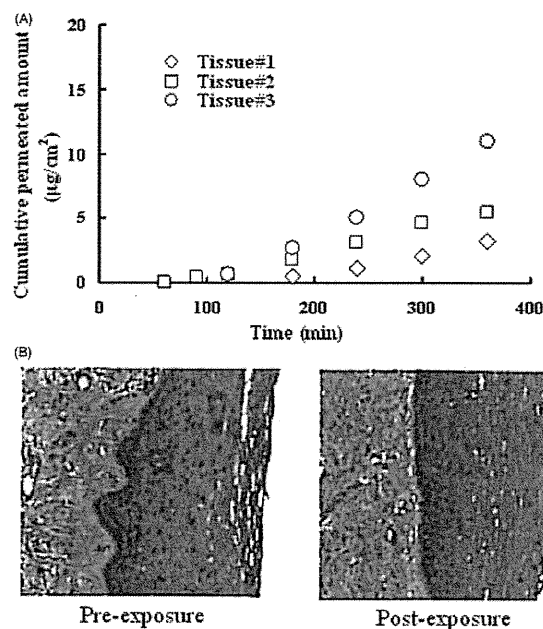


Figure 8. (A) The cumulative amount of EFdA transported through the tissue versus time obtained from permeability experiments with 3 different fresh human ectocervical tissues. (B) Comparison of morphology of human ectocervical tissues pre- and post-treatment.

tissues exposed to EFdA suggests the low tissue toxicity of EFdA (Figure 8B).

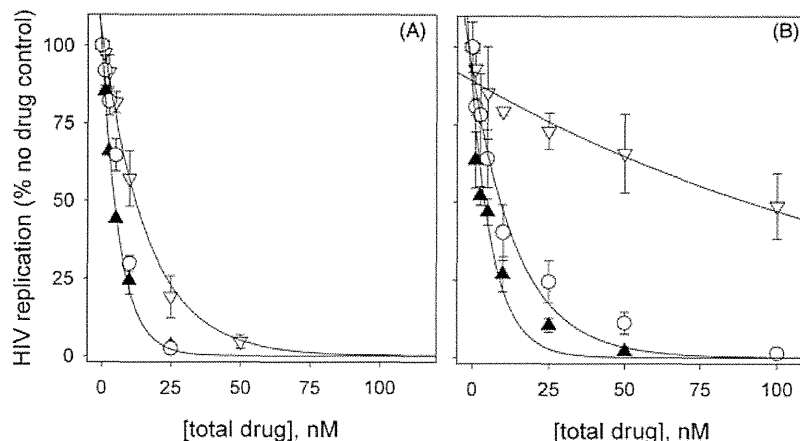
### Bioactivity analysis

UC781 was the first potent NNRTI to be considered for use in microbicidal applications<sup>30</sup>. We compared the anti-HIV activity of EFdA to that of UC781 using a cell-based assay that effectively limits HIV replication to a single cycle. Both EFdA and UC781 were found to be highly potent inhibitors under conditions in which the drugs remain present at constant levels throughout the HIV infection process (Figure 9A). However, EFdA was found to be about two-fold more potent than UC781 under these conditions. The protective or ‘memory’ effect imparted by EFdA was significantly superior to that of UC781 (Figure 9B). In these experiments, designed to assess the pre-exposure prophylactic activity of microbicide candidates, uninfected cells are exposed to drug, the exogenous drug is then removed and the pretreated cells are exposed to HIV. As seen in Figure 9(B), cells pretreated with EFdA retained anti-HIV protection similar to that seen when EFdA was present throughout the infection (Figure 9A). In contrast, cells pretreated with identical concentrations of UC781 showed substantial diminution of anti-HIV protection as compared to conditions where UC781 was present throughout infection.

### Conclusions

Preformulation studies revealed that EFdA is relatively soluble in water, exists in planar or flaky structure, and has good stability upon exposure to different pH conditions and increased temperature over a period of 21 days. *In vitro* cytotoxicity of EFdA was performed in different human epithelial cell lines, and the cytotoxic profiles for EFdA were found to be dependent on incubation time and cell line origin. Transport studies conducted in Caco-2 cell monolayers suggest that both passive and active transport mechanisms may be involved in bidirectional transport of EFdA. In addition, the apparent permeability coefficient ( $P_{app}$ ) of EFdA was found to be  $8.34 \times 10^{-7}$  cm/s in an excised human

Figure 9. Bioactivity analysis of EFdA ( $\blacktriangle$ ), the NNRTI UC781 ( $\nabla$ ) and an equimolar combination of EFdA + UC781 ( $\circ$ ). Details of the experimental protocol are in Materials and Methods. (A) Antiviral activity. P4R5 cells were simultaneously exposed to HIV-1 and the indicated concentrations of the drug. Drug was maintained in the culture throughout the 48 h infection period. (B) Protective activity or “memory” effect. Uninfected P4R5 cells were preincubated with the indicated concentration of drug for 16 h. The cells were washed free of exogenous drug and then exposed to infectious HIV. No exogenous drug was present throughout the 48 h infection period.



ectocervical tissue permeability study. Taken together, the low cytotoxicity, potent anti-HIV activity, and good stability profile for EFdA provide rationale for the development of this drug substance into an anti-HIV pharmaceutical product.

### Acknowledgements

We gratefully acknowledge the staff associated with the Materials Micro-Characterization Laboratory, Department of Mechanical Engineering and Materials Science, University of Pittsburgh, for assistance with the scanning electron microscopy conducted in this study. We would like to thank Marilyn R. Cost for her technical support in the human tissue processing.

### Declaration of interest

Wei Zhang, Michael A. Parniak, Stefan G. Sarafianos, Phillip W. Graebing and Lisa C. Rohan report no declaration of interest. Hiroaki Mitsuya is a named inventor on patent US 7339053 which describes EFdA and its activity against HIV-1.

Research reported in this publication was supported in part by the National Institute of Allergy and Infectious Diseases of the National Institutes of Health under Award Number AI 076119 and AI 079801. The content is solely the responsibility of the authors and does not necessarily represent the official views of the National Institutes of Health.

### References

- UNAIDS, Global Report: UNAIDS world AIDS day report 2011.
- Hladik F, McElrath MJ. Setting the stage: host invasion by HIV. *Nat Rev Immunol* 2008;8:447–57.
- Rohan LC, Moncla BJ, Ayudhya RP, et al. In vitro and ex vivo testing of tenofovir shows it is effective as an HIV-1 microbicide. *PLoS One* 2010;5:e9310.
- Akil A, Parniak MA, Dezzutti CS, et al. Development and characterization of a vaginal film containing dapivirine, a non-nucleoside reverse transcriptase inhibitor (NNRTI), for prevention of HIV-1 sexual transmission. *Drug Deliv Transl Res* 2011;1:511–17.
- Sassi AB, Cost MR, Cole AL, et al. Formulation development of retrocyclin 1 analog RC-101 as an anti-HIV vaginal microbicide product. *Antimicrob Agents Chemother* 2011;55:2282–9.
- Ham AS, Rohan LC, Boczar A, et al. Vaginal film drug delivery of the pyrimidinedione IQP-0528 for the prevention of HIV infection. *Pharm Res* 2012;29:1897–907.
- Geonotti AR, Katz DF. Compartmental transport model of microbicide delivery by an intravaginal ring. *J Pharm Sci* 2010;99:3514–21.
- Ndesendo VM, Pillay V, Choona YE, et al. In vivo evaluation of the release of zidovudine and polystyrene sulfonate from a dual intravaginal bioadhesive polymeric device in the pig model. *J Pharm Sci* 2011;100:1416–35.
- Moss JA, Malone AM, Smith TJ, et al. Safety and pharmacokinetics of intravaginal rings delivering tenofovir in pig-tailed macaques. *Antimicrob Agents Chemother* 2012;56:5952–60.
- Singer R, Mawson P, Derby N, et al. An intravaginal ring that releases the NNRTI MIV-150 reduces SHIV transmission in macaques. *Sci Transl Med* 2012;4:150ra123.
- Balzarini J, Van Damme L. Microbicide drug candidates to prevent HIV infection. *Lancet* 2007;369:787–97.
- Nakata H, Amano M, Koh Y, et al. Activity against human immunodeficiency virus type 1, intracellular metabolism, and effects on human DNA polymerases of 4'-ethynyl-2-fluoro-2'-deoxyadenosine. *Antimicrob Agents Chemother* 2007;51:2701–8.
- Kawamoto A, Kodama E, Sarafianos SG, et al. 2'-Deoxy-4'-C-ethynyl-2-halo-adenosines active against drug-resistant human immunodeficiency virus type 1 variants. *Int J Biochem Cell Biol* 2008;40:2410–20.
- Michailidis E, Marchand B, Kodama EN, et al. Mechanism of inhibition of HIV-1 reverse transcriptase by 4'-ethynyl-2-fluoro-2'-deoxyadenosine triphosphate, a translocation defective reverse transcriptase inhibitor. *J Biol Chem* 2009;284:35681–91.
- Hattori S, Ide K, Nakata H, et al. Potent activity of a nucleoside reverse transcriptase inhibitor, 4'-ethynyl-2-fluoro-2'-deoxyadenosine, against human immunodeficiency virus type 1 infection in a model using human peripheral blood mononuclear cell-transplanted Nod/SCID janus kinase 3 knockout mice. *Antimicrob Agents Chemother* 2009;53:3887–93.
- Murphey-Corb M, Rajakumar P, Michael H, et al. Response of simian immunodeficiency virus to the novel nucleoside reverse transcriptase inhibitor 4'-ethynyl-2-fluoro-2'-deoxyadenosine in vitro and in vivo. *Antimicrob Agents Chemother* 2009;53:3887–93.
- Sha XY, Fang XL. Transport characteristics of 9-nitrocamptothecin in the human intestinal cell line Caco-2 and everted gut sacs. *Int J Pharm* 2004;272:161–71.
- Leonard F, Collnot EM, Lehr CM. A three-dimensional coculture of enterocytes, monocytes and dendritic cells to model inflamed intestinal mucosa in vitro. *Mol Pharm* 2010;7:2103–19.
- Hubatsch I, Ragnarsson EG, Artursson P. Determination of drug permeability and prediction of drug absorption in Caco-2 monolayers. *Nat Protoc* 2007;2:2111–19.
- Artursson P, Palm K, Luthman K. Caco-2 monolayers in experimental and theoretical predictions of drug transport. *Adr Drug Deliv Rev* 2001;46:27–43.
- Gali Y, Delezay O, Brouwers J, et al. In vitro evaluation of viability, integrity, and inflammation in genital epithelia upon exposure to pharmaceutical excipients and candidate microbicides. *Antimicrob Agents Chemother* 2010;54:5105–14.
- Krebs FC, Miller SR, Catalone BJ, et al. Comparative in vitro sensitivities of human immune cell lines, vaginal and cervical epithelial cell lines, and primary cells to candidate microbicides nonoxynol 9, C31G, and sodium dodecyl sulfate. *Antimicrob Agents Chemother* 2002;46:2292–8.
- Christensen ND, Reed CA, Culp TD, et al. Papillomavirus microbicidal activities of high-molecular-weight cellulose sulfate,

- dextran sulfate, and polystyrene sulfonate. *Antimicrob Agents Chemother* 2001;45:3427–32.
24. Artursson P. Epithelial transport of drugs in cell culture. I: A model for studying the passive diffusion of drugs over intestinal absorptive (Caco-2) cells. *J Pharm Sci* 1990;79:476–82.
  25. Artursson P, Karlsson J. Correlation between oral drug absorption in humans and apparent drug permeability coefficients in human intestinal epithelial (Caco-2) cells. *Biochem Biophys Res Comm* 1991;175:880–5.
  26. Neuhoff S, Ungell AL, Zamora I, Artursson P. pH-dependent bidirectional transport of weakly basic drugs across Caco-2 monolayers: implications for drug–drug interactions. *Pharm Res* 2003;20:1141–8.
  27. Neuhoff S, Ungell AL, Zamora I, Artursson P. pH-dependent passive and active transport of acidic drugs across Caco-2 cell monolayers. *Eur J Pharm Sci* 2005;25:211–20.
  28. Sassi AB, Mccullough KD, Cost MR, et al. Permeability of tritiated water through human cervical and vaginal tissue. *J Pharm Sci* 2004; 93:2009–16.
  29. He YL, Murby S, Warhurst G, et al. Species differences in size discrimination in the paracellular pathway reflected by oral bioavailability of poly (ethylene glycol) and D-peptides. *J Pharm Sci* 1998;87:626–33.
  30. Barnard J, Borkow G, Parniak MA. The thiocarboxanilide nonnucleoside UC781 is a tight-binding inhibitor of HIV-1 reverse transcriptase. *Biochemistry* 1997;36:7786–92.

## Abacavir/Lamivudine versus Tenofovir/Emtricitabine with Atazanavir/Ritonavir for Treatment-naïve Japanese Patients with HIV-1 Infection: A Randomized Multicenter Trial

Takeshi Nishijima<sup>1,2</sup>, Misao Takano<sup>1</sup>, Michiyo Ishisaka<sup>1</sup>, Hirokazu Komatsu<sup>3</sup>, Hiroyuki Gatanaga<sup>1,2</sup>, Yoshimi Kikuchi<sup>1</sup>, Tomoyuki Endo<sup>4</sup>, Masahide Horiba<sup>5</sup>, Satoru Kaneda<sup>6</sup>, Hideki Uchiumi<sup>7</sup>, Tomohiko Koibuchi<sup>8</sup>, Toshio Naito<sup>9</sup>, Masaki Yoshida<sup>10</sup>, Natsuo Tachikawa<sup>11</sup>, Mikio Ueda<sup>12</sup>, Yoshiyuki Yokomaku<sup>13</sup>, Teruhisa Fujii<sup>14</sup>, Satoshi Higasa<sup>15</sup>, Kiyonori Takada<sup>16</sup>, Masahiro Yamamoto<sup>17</sup>, Shuzo Matsushita<sup>2</sup>, Masao Tateyama<sup>18</sup>, Yoshinari Tanabe<sup>19</sup>, Hiroaki Mitsuya<sup>20,21</sup>, Shinichi Oka<sup>1,2</sup>,  
on behalf of the Epzicom-Truvada study team

---

### Abstract

---

**Objective** To compare the efficacy and safety of fixed-dose abacavir/lamivudine (ABC/3TC) and tenofovir/emtricitabine (TDF/FTC) with ritonavir-boosted atazanavir (ATV/r) in treatment-naïve Japanese patients with HIV-1 infection.

**Methods** A 96-week multicenter, randomized, open-label, parallel group pilot study was conducted. The endpoints were times to virologic failure, safety event and regimen modification.

**Results** 109 patients were enrolled and randomly allocated (54 patients received ABC/3TC and 55 patients received TDF/FTC). All randomized subjects were analyzed. The time to virologic failure was not significantly different between the two arms by 96 weeks (HR, 2.09; 95% CI, 0.72-6.13;  $p=0.178$ ). Both regimens showed favorable viral efficacy, as in the intention-to-treat population, 72.2% (ABC/3TC) and 78.2% (TDF/FTC) of the patients had an HIV-1 viral load  $<50$  copies/mL at 96 weeks. The time to the first grade 3 or 4 adverse event and the time to the first regimen modification were not significantly different between the two arms (adverse event: HR 0.66; 95% CI, 0.25-1.75,  $p=0.407$ ) (regimen modification: HR 1.03; 95% CI, 0.33-3.19,  $p=0.964$ ). Both regimens were also well-tolerated, as only 11.1% (ABC/3TC) and 10.9% (TDF/FTC) of the patients discontinued the allocated regimen by 96 weeks. Clinically suspected abacavir-associated hypersensitivity reactions occurred in only one (1.9%) patient in the ABC/3TC arm.

**Conclusion** Although insufficiently powered to show non-inferiority of viral efficacy of ABC/3TC relative to TDF/FTC, this pilot trial suggested that ABC/3TC with ATV/r is a safe and efficacious initial regimen for HLA-B\*5701-negative patients, such as the Japanese population.

---

<sup>1</sup>AIDS Clinical Center, National Center for Global Health and Medicine, Japan, <sup>2</sup>Center for AIDS Research, Kumamoto University Graduate School of Medical Sciences, Japan, <sup>3</sup>Department of Community Care, Saku Central Hospital, Japan, <sup>4</sup>Department of Hematology, Hokkaido University Hospital, Japan, <sup>5</sup>Division of Respiratory Medicine, Higashisaitama National Hospital, Japan, <sup>6</sup>Department of Gastroenterology, National Hospital Organization Chiba Medical Center, Japan, <sup>7</sup>Department of Medicine and Clinical Science, Gunma University Graduate School of Medicine, Japan, <sup>8</sup>Department of Infectious Diseases and Applied Immunology, Research Hospital of the Institute of Medical Science, The University of Tokyo, Japan, <sup>9</sup>Department of General Medicine, Juntendo University School of Medicine, Japan, <sup>10</sup>Department of Infectious Diseases and Infection Control, The Jikei University School of Medicine, Japan, <sup>11</sup>Department of Infectious Diseases, Yokohama Municipal Citizen's Hospital, Japan, <sup>12</sup>Immunology and Infectious Disease, Ishikawa Prefectural Central Hospital, Japan, <sup>13</sup>Clinical Research Center, National Hospital Organization Nagoya Medical Center, Japan, <sup>14</sup>Division of Blood Transfusion, Hiroshima University Hospital, Japan, <sup>15</sup>Division of Hematology, Department of Internal Medicine, Hyogo College of Medicine, Japan, <sup>16</sup>Postgraduate Clinical Training Center, Ehime University Hospital, Japan, <sup>17</sup>Internal Medicine, Clinical Research Institute, National Hospital Organization Kyushu Medical Center, Japan, <sup>18</sup>Department of Infectious, Respiratory, and Digestive Medicine Control and Prevention of Infectious Diseases Faculty of Medicine, University of the Ryukyus, Japan, <sup>19</sup>Division of Infection Control and Prevention, Niigata University Medical and Dental Hospital, Japan, <sup>20</sup>Departments of Infectious Diseases and Hematology, Kumamoto University Graduate School of Medical Sciences, Japan and <sup>21</sup>Experimental Retrovirology Section, HIV and AIDS Malignancy Branch, National Cancer Institute, National Institutes of Health, USA

Received for publication October 18, 2012; Accepted for publication December 17, 2012

Correspondence to Dr. Shinichi Oka, oka@acc.ncgm.go.jp